U.PORTO

FMUP FACULDADE DE MEDICINA
UNIVERSIDADE DO PORTO

Effect of SPRR1A overexpression on the nociceptive behaviour of OA animals

Raquel Marinho do Nascimento Alonso

M

2017

Departamento de Biomedicina
Unidade de Biologia Experimental
Faculdade de Medicina da Universidade do Porto

Master in Neurobiology

Supervisor: Professora Doutora Joana Ferreira-Gomes
Co-supervisor: Professora Doutora Fani Neto

Agradecimentos

À minha orientadora, Doutora Joana Ferreira-Gomes, e co-orientadora, Doutora Fani Neto, a minha enorme gratidão pela amizade, simpatia, carinho, disponibilidade, por todas as palavras de conforto e por todo o conhecimento e sabedoria transmitidos

Ao Doutor Carlos Reguenga por toda ajuda, partilha de conhecimento e paciência.

À Doutora Diana Nascimento, por me ter ensinado grande parte do que sei, por toda a boa disposição, amizade e carinho.

A todos os meus colegas do mestrado e do departamento, Rita Costa, Zé Tiago, Raquel Oliveira, Marta, Joana Bravo, Joana Augusto, Ricardo, Helena, Rita Oliveira, Inês, Rafa, Diana Correia, Sílvia, Zé Carlos e Raquel Silva, um enorme obrigada por todos os momentos partilhados. Um especial obrigada, aos meus colegas de gabinete, Zé Carlos e Raquel Silva, pela amizade e paciência e à Lenita, pelo companheirismo e por me acalmar nos momentos mais difíceis.

Aos meus pais, pois sem eles esta caminhada não teria sido possível. Ao Afonso, por todo o amor e compreensão.

Abstract

Osteoarthritis (OA) is a highly common articular disease whose prevalence is associated with several risk factors, like age, obesity, genetic predisposition and prior joint injury. Chronic pain is the most striking symptom of this condition, being the main complaint presented by patients, therefore, the main clinical concern is its treatment. OA is considered an inflammatory and nociceptive disease but recent studies have been pointing towards the possibility of a neuropathic component in the mechanisms of pain associated with the disease. Indeed, studies from our group using both the monoiodoacetate- (MIA) and the collagenase-induced models of OA have found an increase in the number of primary afferent neurons expressing markers of neuronal damage, in ipsilateral dorsal root ganglia (DRG). In both models an increased expression of regeneration associated-genes (RAGs) was also observed. In the collagenase-induced OA model a significant increase in the expression of the RAG small proline rich protein 1A (SPRR1A) was observed. Taking into account these findings, we investigated the potential contribution of SPRR1A overexpression on the nociceptive behaviour of OA animals.

For this purpose, a viral vector engineered to express SPRR1A (AAV2/5-SPRR1A) was intra-ganglionically injected in OA and control animals. Besides it, AAV2/5 expressing Green Fluorescent Protein (AAV2/5-GFP) and saline were as well injected in DRG of other groups of animals. During the following 4 weeks the animals´ nociceptive behaviour was assessed trough the Von Frey, CatWalk and Knee-Bend tests, as well their motor coordination, by using the rotarod test. Indeed, OA animals injected with AAV2/5-SPRR1A revealed attenuation in their nociception and gene expression studies confirmed the great increase of SPRR1A mRNA levels in the DRG of control and OA animals. However, an unequal SPRR1A expression was found, with ipsilateral DRG of control animals revealing a much greater overexpression. ATF-3 and GFAP mRNA levels showed as well a higher increase in the ipsilateral DRG of control animals following AAV2/5-SPRR1A injection. The knees of these animals showed a slight erosion of the cartilage and consequent exposure of the subchondral bone, detected by histological analysis. The animals injected with AAV2/5-GFP or saline showed minor nociceptive behaviours due to the intra-ganglionic surgery procedure, which were progressively resolved after the first week

following injection. Additionally, although OA animals injected with AAV2/5-GFP or saline have shown the maintenance of nociceptive behaviours, their ipsilateral DRG, as well those of control animals, showed high levels of SPRR1A mRNA, probably due to the highly invasive surgical procedure.

Data suggest SPRR1A plays an important role in the peripheral events leading to the development of nociceptive behaviour in experimental models of OA. Targeting its expression in the DRG, namely by enhancing it, might be a potential approach for pain attenuation, possibly by promoting regenerative mechanisms within the sensory ganglia. However, further studies are still necessary to evaluate the molecular mechanisms behind SPRR1A role and to develop less invasive delivery routes for gene targeting in the DRG.

Keywords: Osteoarthritis (OA), Dorsal root ganglia (DRG), Regeneration-associated genes (RAGs), small proline rich protein 1A (SPRR1A), AAV2/5-SPRR1A, intra-ganglionic injection

Resumo

A osteoartrose (OA) é uma doença articular extremamente comum cuja prevalência está associada a vários fatores, como idade, predisposição genética e existência de lesão articular anterior. A dor crónica é o sintoma mais marcante desta condição, sendo também o que é mais reportado pelos doentes, pelo que a maior preocupação clínica é o seu tratamento. A OA é considerada uma doença inflamatória e nocicetiva mas estudos recentes têm apontado para a possibilidade de um componente neuropático nos mecanismos da dor associados a esta patologia. De facto, estudos do nosso grupo usando a injeção de monoiodoacetato (MIA) e colagenase como modelos de indução da OA encontraram um aumento no número de neurónios aferentes primários que expressam marcadores de lesão neuronal, nos gânglios raquidianos ipsilaterais. Em ambos os modelos foi também observada uma expressão aumentada de genes associados à regeneração (RAG, de *regeneration associated-genes*). No modelo de OA induzido pela colagenase foi observado um aumento significativo da expressão da pequena proteína 1A rica em prolina (SPRR1A, de *small proline rich protein 1A*), que pertence à família dos RAG. Tendo em conta estes dados, nós investigámos o potencial efeito da sobreexpressão do SPRR1A no comportamento nocicetivo de animais com OA.

Para este efeito, um vector viral construído para expressar SPRR1A (AAV2/5-SPRR1A) foi injetado intra-ganglionicamente em animais OA e controlo. Além disso, AAV2/5-GFP (de *green fluorescent protein*, ou proteína florescente verde) ou solução salina foram também injetados no DRG de outros grupos de animais. Durante as 4 semanas seguintes o comportamento nocicetivo dos animais foi avaliado através dos testes de Von Frey, CatWalk e Knee-Bend, assim como a sua coordenação motora, usando o teste rotarod. De facto, os animais OA injetados com AAV2/5-SPRR1A apresentaram uma atenuação da sua nociceção e estudos de expressão génica confirmaram o grande aumento nos níveis de mRNA para o SPRR1A no DRG de animais OA e animais controlo. No entanto, uma expressão desigual de SPRR1A foi encontrada, com os DRG ipsilaterais dos animais controlo a revelarem uma sobreexpressão muito maior. Os níveis de mRNA para o ATF-3 e GFAP mostraram também um maior aumento nos DRG ipsilaterais dos animais controlo após injeção de AAV2/5-SPRR1A. Os joelhos destes animais mostraram uma ligeira erosão da cartilagem e consequente exposição do osso subcondral, detetada por técnicas

histopatológicas. Os animais injetados com AAV2/5-GFP ou solução salina mostraram comportamentos nocicetivos menos acentuados devido ao procedimento cirúrgico intra-ganglionar. No entanto, esta nociceção foi progressivamente resolvida após a primeira semana após a injeção. Para além disso, apesar dos animais OA injetados com AAV2/5-GFP ou solução salina terem mostrado comportamentos nocicetivos permanentes, os seus DRG ipsilaterais, assim como os dos animais controlo, mostraram níveis elevados de mRNA para o SPRR1A, provavelmente devido ao procedimento cirúrgico extremamente invasivo.

Os dados sugerem que o SPRR1A tem um papel importante em eventos periféricos que conduzem ao desenvolvimento do comportamento nocicetivo em modelos experimentais de OA. Alvejar a sua expressão no DRG, nomeadamente aumentando-a, pode ser uma potencial abordagem para atenuar a dor, possivelmente promovendo mecanismos regenerativos dentro dos gânglios sensitivos. No entanto, novos estudos ainda são necessários para avaliar os mecanismos moleculares subjacentes ao papel do SPRR1A e para desenvolver vias de administração menos invasivas para alvejar genes no DRG.

Palavras-Chave: Osteoartrose (OA), Gânglios raquidianos (DRG), genes associados à regeneração (RAGs), pequena proteína 1A rica em prolina (SPRR1A), AAV2/5-SPRR1A, injeção intra-ganglionar.

Table of contents

List of figures

List of tables

List of abbreviations

AAV	Adeno-associated virus
ACLT	Anterior Cruciate Ligament Transection
AIA	Adjuvant-Induced Arthritis
ATF-3	Activating Transcription Factor 3
BASP1	Brain Acid Soluble Protein 1
BDNF	Brain-derived Neurotrophic Factor
BME	Bone Marrow Edema
BML	Bone Marrow Lesions
BP	Benzoyl Peroxide
CGRP	Calcitonin Gene-Related Peptide
CNS	Central Nervous System
CSF	Cerebrospinal Fluid
DF	Dibutyl Phthalate
DRG	Dorsal Root Ganglia
DMM	Destabilization of the Medial Meniscus
FRAP	Fluoride-Resistant Acid Phosphatase
GAP-43	Growth-associated Protein 43
GAPDH	Glyceraldehyde-3-Phosphate Dehydrogenase
GFAP	Glial Fibrillary Acidic Protein
GFP	Green Fluorescence Protein
HL	Hind Limb
IA OC fragment	Intra-articular Osteochondral Fragment
IASP	International Association for the Study of Pain
IB4	Isolectin B4
IL-1	Interleukin-1
IL-6	Interleukin-6
IL-17	Interleukin-17
MCLT	Medial Collateral Ligament Transection
MIA	Monoiodoacetate
MM	Medial Meniscectomy
MMA	Methyl Methacrylate Resin
MMT	Medial Meniscal Transection

MRI	Magnetic Resonance Imaging
NF-200	Neurofilament 200
NGF	Nerve growth factor
NGS	Normal Goat Serum
NT-3	Neurotrophin 3
NPY	Neuropeptide Y
NSAIDs	Non-steroidal Anti-inflammatory Drugs
OA	Osteoarthritis
PBS	Phosphate-buffered saline
PBST	PBS with Triton x-100
PNI	Peripheral Nerve Injury
PNS	Peripheral Nervous System
PWT	Paw Withdrawal Threshold
rAAV	Recombinant Adeno-Associated Vector
RAGs	Regeneration-Associated Genes
SOX11	SRY (sex determining region Y)-box11
SP	Substance P
SPRR1A	Small Proline Rich Protein 1A
TANK	TRAF Family Member-Associated NFKB Activator
TIPPI	Total Ipsilateral Paw Print Intensity
TrkA	Tyrosine kinase A

Introduction

1.Pain

1.1 Pain definition

The pain term was subject to a lot of controversy for many years due to the complexity of the sensation. To overcome this disagreement, in 1994 the International Association for the Study of Pain (IASP), defined pain as "an unpleasant sensory and emotional experience associated with actual or potential tissue damage, or described in terms of such damage" (Merskey and Bogduk, 1994). From this definition stands out that pain has an individual connotation, since it combines the sensory perception with an unpleasant emotional experience, which demonstrates its subjectivity. While the sensory component allows describing the noxious stimulus in regard to the time, space, intensity and physical qualification, the emotional component is responsible for the behavioural response to pain (Walk & Poliak-Tunis, 2016).

Though undesirable, pain acts as a warning system, having an important biological function, as it is necessary for the maintenance of the body homeostasis (Gibson & Farrell, 2004). Nonetheless, pain often outlives its protective utility, when it becomes chronic, persisting after acute injury and causing alterations in the pain pathway.

1.2 Pain transmission

In 1906, Sherrington proposed that the detection of noxious stimuli is done by nociceptors (Sherrington, 1906). These are high-threshold sensory receptors of the peripheral nervous system (PNS) capable of transducing mechanical, chemical and thermal noxious stimuli from different organism locations, like skin, muscles, viscera and joints, into action potentials. The cell bodies of these neurons are located at sensory ganglia, namely trigeminal ganglia, for stimuli occurring in the face and head, and dorsal root ganglia (DRG) for stimuli arriving from the remaining body. Each cell body possesses a unique axon which bifurcates in two branches. One of the branches, the central, projects to the dorsal horn of the spinal cord while the peripheral branches terminate in many peripheral organs constituting the sensitive fibres. There are 3 types of fibres and they are distinguished according to their diameter, myelination degree and conduction velocity (Aβ, Aδ and C) (Fig. 1) (Castro-Lopes & Neto, 2003). Aβ fibres do not contribute to acute pain, once they only detect innocuous stimuli, but they have the largest diameter, conduct the information faster and are myelinated. On

the other hand, Aδ and C fibres are responsible for transmitting the nociceptive information. While Aδ fibres are thinly myelinated, have medium diameter and carry information more rapidly, C fibres are unmyelinated, have small diameter and carry information very slowly. Furthermore, Aδ nociceptors are responsible for the more acute and rapid pain sensation, and C nociceptors for the more diffuse and prolonged pain (Julius & Basbaum, 2001).

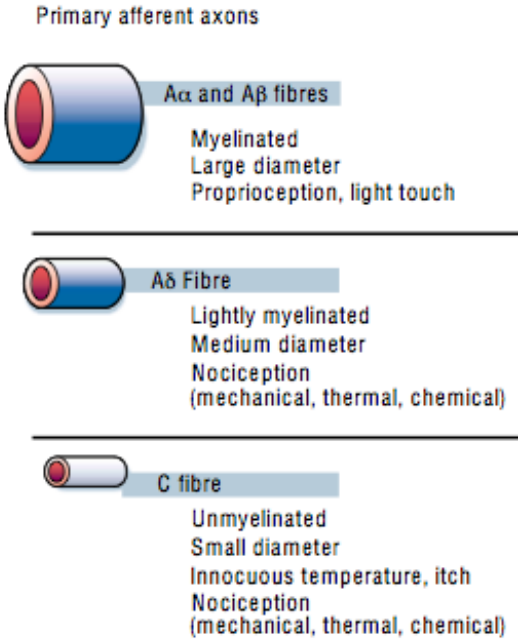

Figure 1. Sensitive fibres. Differences between sensitive fibres regarding to diameter, myelination degree and the type of the information they lead (Julius & Basbaum, 2001).

In short, noxious stimuli activate the nociceptors, which in turn generate excitatory impulses that travel through sensory afferent axons to the dorsal horn of the spinal cord and from there to supraspinal sites in the central nervous system (CNS). In the various supraspinal regions, the information is processed, modulated and integrated with cardiovascular-, emotional- and cognitive-related information, resulting in the overall pain sensation (Fig. 2) (Bingham *et al.*, 2009)

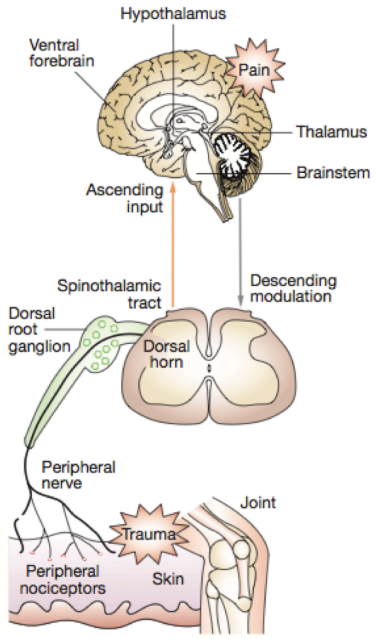

Figure 2. The nociceptive pain pathway. Activation of peripheral pain receptors (nociceptors) by noxious stimuli generates signals that travel through peripheral nerves to the cell bodies of primary afferent neurons located at sensory ganglia, such as dorsal root ganglia in the case of stimuli arriving from the skin or joints. From there, the action potentials are transmitted to the dorsal horn of spinal cord via the primary afferent neurons' central axonal branch. From the dorsal horn, the inputs are carried to upper regions in the CNS through various ascending tracts, such as the spinothalamic tract, where they are processed and integrated, generating the pain sensation. Descending inhibitory and facilitatory supraspinal projections to the spinal cord modulate the quality of the signal that is processed at the spinal cord and transmitted to supraspinal regions (Bingham *et al*., 2009).

1.3 Pain Classification

Pain might be classified according to its duration. It may have a protective role and, if so, it is called acute pain. This type of pain works as an awareness alert in order to avoid possible damages on the organism, serving as the boost to avoid the source of damaging stimuli or to seek health care. Furthermore, this pain has limited duration since it ends when the underlying injury is solved (Cousins & Power, 1999). On the other hand, when pain becomes repetitive and long lasting it loses the warning function of physiologic nociception, and it becomes pathological itself, being called chronic pain (Fishman *et al*., 2010). According to IASP, chronic pain is defined as lasting for more than 6 months. Estimates suggest that 1 in 10 adults are diagnosed with chronic pain each year making pain a serious medical problem (Goldberg &

McGee, 2011). It is associated with poor quality of life and high personal, social and financial burden.

Pain can also be classified according to its cause and the place where it originates. In agreement, pain is currently classified into neuropathic or nociceptive. According to IASP, neuropathic pain is defined as " pain caused by a lesion or disease of the somatosensory system" (Merskey and Bogduk, 1994). Neuropathic pain is not a single disease, but a condition that may be triggered by many causes, such as diabetes, surgery or trauma, stroke or spinal cord injury; however, sometimes the cause is unknown (Jensen *et al.*, 2011; Cooper *et al.*, 2017). Neuropathic pain conditions are associated with two symptoms that stand out, namely allodynia, defined as pain elicited by a stimulus that normally does not cause pain, and hyperalgesia, an increased sensitivity to a stimulus that normally already causes pain. Contrary to neuropathic pain, nociceptive pain occurs with a normally functioning somatosensory nervous system, being defined as "pain that arises from actual or threatened damage to non-neural tissue and is due to the activation of nociceptors" (Nicholson, 2006).

2. Osteoarthritis

2.1 Characteristics of Osteoarthritis

Osteoarthritis is considered the most common form of articular disease whose major symptom is chronic pain. It is known that the prevalence of OA increases with age, with notable differences between men and women, with women having higher rates than men. Beyond age and gender, obesity, genetic predisposition and prior joint injury are also risk factors for OA. Among all types of OA, knee osteoarthritis is the most incident (Oliveira *et al.,* 1995) and this high prevalence has a great impact on physical functioning and quality of life. Therefore, identifying approaches to its prevention should be a public health priority (Blagojevic *et al.*, 2010).

OA diseases are a result of both mechanical and biological events and are associated with the progressive degeneration of the articular cartilage (Forsey *et al.*, 2006). Articular cartilage is an avascular tissue that coats the ends of bones and has as prime functions to support and distribute forces during joint loading (Mow *et al.*, 1992). The matrix of articular cartilage is saturated with water being composed by chondrocytes, proteoglycans and collagen. Chondrocytes are the only cells that exist in the matrix and their function is to regulate the synthesis and degradation processes of the matrix components. Both proteoglycans and collagen are proteins and their

main functions are to give rigidity to the matrix and to confer tensile strength to cartilage, respectively (Martel-Pelletier *et al.*, 2012).

OA appears when there is an imbalance between these synthesis and degradation activities, resulting in loss of cartilage matrix components. As consequence, the cartilage becomes weaker and, thus, more susceptible to mechanical injury leading to chondrocytes death (Goldring, 2000; Pritzker *et al.*, 2006). Nevertheless, in the early stages of the disease, there are attempts by the cartilage to regenerate and to produce new tissue, namely fibrocartilage. Despite this, the failure of an adequate response of repair to injury results in irreversible changes (Lohmander et al., 1994). Although it seems that initially OA affects mainly the cartilage, the entire joint is involved, including the subchondral bone, ligaments, capsule, and synovial membrane (Martel-Pelletier *et al.*, 2012).

2.2 Inflammatory component on osteoarthritic pain

Initially, OA has been defined as a non-inflammatory disease, but features of inflammation have been demonstrated during OA progression. Swelling and stiffness of the joint, synovitis (inflammation of the synovium), increases in the number of cytokines and in the number of immune cells are some of the inflammatory characteristics associated with OA (Goldring & Otero, 2011), as shown in Fig.3. Joint swelling and stiffness are clinical signs observed in OA patients reflecting the presence of synovitis, which is characterized by hyperplasia of the synovium and by an infiltration of T and B lymphocytes (Scanzello & Goldring, 2012). Additionally, the dysfunctionality of chondrocytes, which characterizes this disease, results in the production of inflammatory mediators, and of pro-inflammatory cartilage degradation products that perpetuate the inflammatory response. Cytokines, including interleukins 1 (IL-1), 6 (IL-6) and 17 (IL-17), and tumour necrosis factor alpha (TNF-α), are some of the inflammatory mediators that can be identified in the synovial fluid, cartilage and synovium of OA patients (Scanzello *et al.*, 2009; Martel-Pelletier *et al.*, 2016). Thus, the inflammation suggested by these clinic signs might contribute to the pathogenesis of OA, and explain some of the OA symptomatology, namely the pain-associated to this condition.

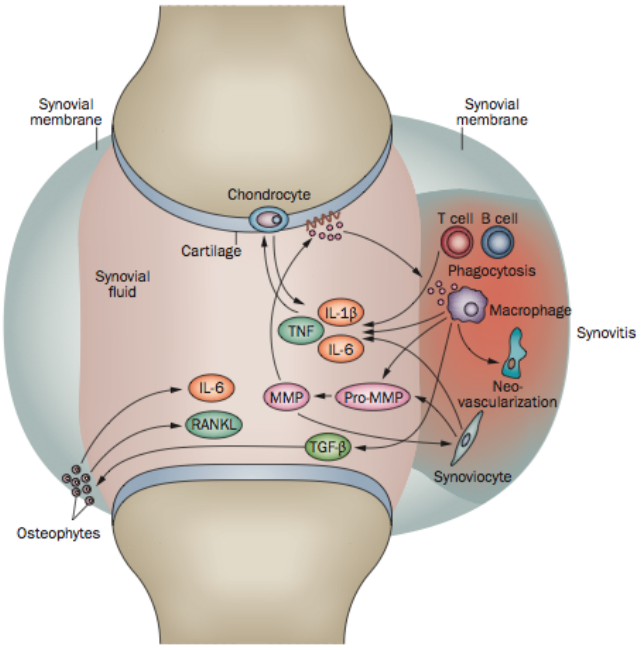

Figure 3. Inflammatory process in OA. Cytokine production (IL-1β, TNF-α and IL-6) and synovitis demonstrated by infiltration of T and B lymphocytes, and macrophages are involved in the inflammatory process of OA (Chevalier et al., 2013). Abbreviations: MMP, matrix metalloproteinase; RANKL, receptor activator of nuclear factor ϰB ligand, also known as tumor necrosis factor ligand superfamily member 11; TGF-β, transforming growth factor β; IL-1B, interleukin1 beta; IL-6, interleukin 6; TNF, tumor necrosis factor.

2.3 Neuropathic and nociceptive components on osteoarthritic pain

During inflammation the peripheral nerve terminals are sensitized by inflammatory mediators, involving changes in joint nociceptors. For this reason, osteoarthritic pain has for long been considered as nociceptive pain (Schaible *et al.*, 2009). However, several studies suggested the presence of a non-nociceptive pain component associated with abnormally excitable pain pathways in the peripheral and the central nervous systems (Valdes *et al.*, 2014). Thus, the presence of somatosensory abnormalities, like mechanical and thermal hyperalgesia, allodynia and referred pain, contributed to the notion that neuropathic pain mechanisms might be involved in osteoarthritic pain. These characteristics may be useful in the clinical assessment to distinguish neuropathic pain from nociceptive pain and for this, screening questionnaires, such as PainDETECT are used. Through the use of this questionnaire in one cohort of patients with knee OA, 34% revealed signs of neuropathy, including burning, tingling or numbness (Hochman *et al.*, 2013; Valdes *et al.*, 2014). Apart from the clinical evidences, several experimental studies

demonstrated there is an increase of markers of nerve injury in sensory nerves innervating the knee of OA rats. Indeed, it was shown that activating transcription factor 3 (ATF-3) and neuropeptide Y (NPY), both markers of neuronal injury, are highly expressed in DRG neurons after OA induction by MIA (Ivanavicius *et al.*, 2007; Ferreira-Gomes *et al.*, 2012b) and collagenase (Adaes *et al.*, 2015). These molecular evidences corroborate the involvement of neuropathic pain events in OA, suggesting that OA pain may come from both nociceptive- and neuropathic-like mechanisms.

3. Osteoarthritic Knee Pain

3.1 Osteoarthritic pain source

The main sensation attributed to the joint is pain, being extremely difficult to understand its source. However, as the cartilage is avascular and aneural, damaged cartilage cannot generate pain directly (Felson, 1990). Therefore, pain must be arising from other structures that are richly enervated such as the subchondral bone, periosteum, periarticular ligaments, periarticular muscles, synovium and joint capsule (Salaffi *et al.*, 2014), as shown in Fig. 4.

In order to evaluate all structures in a joint and identify structural abnormalities, and possibly correlate them with OA pain, magnetic resonance imaging (MRI) might be used. In this regard, subchondral microfratures, bone stretching with lifting of the periosteum due to the formation of osteophytes, joint capsule distension and synovial inflammation are some of the causes proposed as sources of pain in OA (Felson *et al.*, 2001; Schaible, 2012). It has also been shown that anatomical changes such as bone marrow lesions (BML) (Felson *et al.*, 2001), sub-articular bone attrition (Hill *et al.*, 2001), synovitis, and effusion (Hill *et al.*, 2001; Hill *et al.*, 2007) are related to knee pain. Indeed, Felson et al showed a high incidence of bone marrow edema (BME) in 78% of patients with OA knee pain against 30% of non-painful knee OA patients (Schaible, 2012). Furthermore, similar results were found regarding articular lesions, knee effusions and synovitis, since these features have been most frequently found in patients with knee pain than in patients with knee OA but without pain (Hill *et al.*, 2001; Hill *et al.*, 2007)

It has been suggested that the growth of new blood vessels, or angiogenesis, may contribute to OA pain (Ashraf & Walsh, 2008). During the course of OA there is the formation of new cartilage that is invaded by newly formed blood vessels with the

presence of sensory nerves. These nerve terminals mediate a sustained burning pain commonly described by patients with OA (Ashraf & Walsh, 2008). Furthermore, other OA features, such as articular cartilage loss, synovial inflammation, fibrosis, subchondral bone remodelling and osteophyte formation, may be perpetuated by angiogenesis.

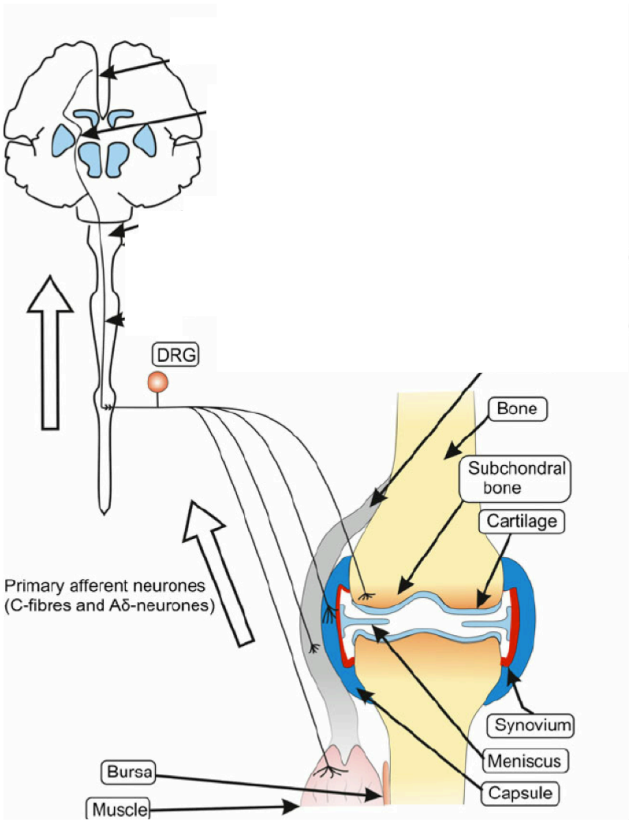

Figure 4. Innervation of a typical articular joint. Tissues such as subchondral bone, joint capsule and synovium receive afferent innervations including C and Aδ fibres (Staunton et al., 2013)

3.2 Innervation on the joint

The knee joint is richly innervated by both sensory and sympathetic peripheral nerve fibres, of which about 80% are unmyelinated. The major function of sensory nerves is to detect and convey mechanical information from the joint to the CNS. Sensory thick myelinated Aβ fibres are thought to transmit information about movement and position of the joint and about pressure exerted on articular tissues. However, knee joints are mostly innervated by nociceptive afferent nerve fibres, namely thinly myelinated Aδ-fibres and unmyelinated C-fibres. Sensory thick myelinated Aβ fibres are equipped with corpuscular Ruffini-, Golgi- and Pacini- type endings and they are found in ligaments, fibrous capsule, menisc and adjacent

periosteum, while thinly myelinated Aδ-fibres and unmyelinated C-fibres terminate as free nerve endings in the same sites of thick myelinated fibres and also in the adipose tissue (Schaible & Grubb, 1993).

Articular afferents have been classified into different groups according to their electrophysiological characteristics. Thick myelinated fibres are activated by innocuous movements, such as by touch, making them low threshold fibres. C- and Aδ-fibres have a higher mechanical threshold and are often activated by noxious manipulations, as, flexion and/or extension and rotations of the joint beyond the normal working range (Schaible & Grubb, 1993; Scaible & Schmidt, 1983).

In sum, two types of sensory fibres innervate knee joints, the high-threshold fibres that may be considered as nociceptive units since they lead to pain sensations, and the low threshold fibres that are considered proprioceptive (Schaible & Grubb, 1993).

3.3 Sensory neurons

The cell bodies of the primary sensory neurons with fibres innervating the joints are located in the PNS, namely in the DRGs. Besides sensory neurons, which are pseudounipolar and innervate several structures, the DRGs contain other cell types such as glial cells, endothelial cells and macrophages (Berta *et al.*, 2017). Glial cells might be of two types, Schwann cells, and satellite glial cells (SGCs). Schwann cells might be myelinating, wrapping around the axons of motor and sensory neurons to form the myelin sheath, or non-myelinating, while SGCs surround the cell bodies and proximal part of the axon forming with the sensory neuron an anatomical and functional neuron-SGC unit. SGCs in sensory ganglia might be visualized by immunolabelling with glutamine synthase, which they produce in basal conditions, and glial fibrillary acidic protein (GFAP) whose expression is upregulated when these cells become activated by stressful or damaging environments to the ganglia or to the sensory neurons, including inflammation and peripheral nerve injury (Hanani, 2005).

The primary sensory neurons in DRGs are categorized into different populations with distinct characteristics in what concerns the size of their cell bodies, the stimuli they are sensitive to, and their neurochemistry. The C nociceptors usually have the smaller cell size and most are polymodal, that is, are sensitive to mechanical, chemical and thermal stimuli. However, there are some of them that are sensitive to thermal and chemical stimuli (mechano-insensitive nociceptors), others that are

sensitive only to chemical stimuli and still others that are sensitive only to thermal stimuli (Belmonte & Cervero, 1996). Beyond this, C nociceptors are referred to as silent nociceptors when they only respond to stimuli in the presence of an injury (Schmidt *et al.*, 1995). Concerning the Aδ nociceptors, they are usually of medium cell size and there are two main classes. Type I respond to both mechanical and chemical stimuli, and despite having high heat thresholds, if the heat stimulus is maintained, these afferents became sensitized and respond at lower temperatures. Type II Aδ nociceptors respond predominantly to thermal stimuli and have a very high mechanical threshold (Basbaum *et al.*, 2009). Regarding the neurochemistry, nociceptors are once again divided into groups. Glutamate is the predominant excitatory neurotransmitter in all nociceptors. C-fiber nociceptors are then separated into two subtypes, peptidergic and non-peptidergic. The peptidergic type have the ability to produce neuropeptides like substance P (SP) and calcitonin gene-related peptide (CGRP), and express TrkA neurotrophin receptor, which responds to neuronal growth factor (NGF) (Belmonte & Cervero, 1996). The non-peptidergic type can be identified by the presence of enzymes (FRAP-Fluoride-resistant acid phosphatase) and binding sites for the isolectin-B4 (Belmonte & Cervero, 1996). Finally, Aδ nociceptors are identified by the presence of certain filaments, such as neurofilament protein (NF200) (Belmonte & Cervero, 1996).

CGRP and SP have been shown to be expressed in joint afferents (O'Brien *et al.*, 1989). In the MIA model of OA, an increased expression of SP and CGRP has been found in neurons innervating the knee joint (Ahmed *et al.*, 2012). Furthermore, since these neurotransmitters migrate to nerve terminals of primary afferent neurons, SP and CGRP were found increased as well in the synovium in a rat anterior cruciate ligament transection model of OA (Yoshida *et al.*, 2012). So, this marked increase in the production of neuropeptides after OA development may be involved in joint pain processing. Through retrograde labeling with fluorogold injected into the knee it has been reported that non-peptidergic nerve fibres (IB4-positive) are present at very low levels in the rat knee joint of control rats and this was not significantly different from the percentage found in rats with OA induced by MIA (Ferreira-Gomes *et al*., 2010). Similarly, in the same study, it was found a large percentage of NF-200 positive backlabeled cells in the DRGs neurons innervating the knee joint with no differences between control and OA rats (Ferreira-Gomes *et al.,* 2010).

In non-physiological conditions, for example in inflammatory or neuropathic pain models, neurochemical and anatomical changes can occur in Aβ neurons. In these conditions Aβ neurons begin to synthesize substances involved in pain sensation which may lead to their hypersensitization and to the acquired ability of being activated by higher threshold stimuli they would normally not transduce. In rats with OA, Ferreira-Gomes et al showed for the first time the alteration of the cell size distribution pattern of CGRP-positive neurons, where large cells started to express CGRP, suggesting a phenotypic switch of these cells has occurred to assume the characteristics of nociceptors (Ferreira-Gomes *et al.,* 2010).

3.4 Treatments available for osteoarthritic pain

Current management of OA pain remains unsatisfactory for many patients, both in terms of providing pain relief, and in terms of producing undesirable side effects (Malfait & Schnitzer, 2013). Different types of interventions are used in an attempt for pain control and current treatment guidelines recommend the use of opioids, non-steroidal anti-inflammatory drugs (NSAIDs), paracetamol and intra-articular therapy with glucocorticoid and hyaluronan preparations (Rhon, 2008; Malfait & Schnitzer, 2013). Some patients show pain relief and increased joint function, but also several side effects. Problems on gastrointestinal, renal, hepatic and cardiovascular systems are some of the complications associated with these therapies (Watson *et al.*, 2000; Crofford, 2013). There are, however, a number of patients, where current drug regimens fail to achieve efficacy, which justifies the necessity to develop new therapies targeting the nociceptive and neuropathic pain mechanisms involved.

4. Experimental osteoarthritis

4.1 Animal models in Osteoarthritis

The lack of an effective OA treatment reflects the need for a better understanding of the pathophysiology and aetiopathology of this joint disease. However, since human clinical studies present several limitations and difficulties, the use of animal models became extremely important (Abramson & Attur, 2009; Vincent *et al.*, 2012). Although there are several OA animal models, there is still no one that is ideal, as they should mimic as much as possible the different complex features observed in OA patients (Abramson & Attur, 2009). Limitations are mostly due to differences in anatomy, dimensions, biomechanics, cartilage repair processes and

cartilage thickness between animal and human joints. Therefore, as each model mimics different OA features, it is necessary the use of several to cover the full range of alterations that characterize OA.

The majority of animal model studies focus on elucidating mechanisms underlying damage to joint structures, while the study of OA pain was, for many years, forgotten (Brandt, 2002). However, more recent studies have been focusing on the development of animal models that best mimic OA pain (Havelin *et al.*, 2016; Otis *et al.*, 2016). OA models can be spontaneous (naturally occurring), genetically modified or chemically- and surgically-induced (Tables 1); yet, chemical-induced models are the most used in OA pain studies.

Animal models	Species	Outcome measures
Spontaneous		
Age-associated	Guinea pig	Mechanosensitivity (EP)
Obesity	Mouse	Grip strength meter, motor coordination (rotarod), gait analysis, spontaneous locomotor activity
Genetic modification		
IL1B over expression	Rat	Thermal hyperalgesia, mechanical allodynia (VF), gait analysis (CatWalk), foot printing, HL weight distribution, treadmill
Col9a1 (_/_)	Mouse	Motor coordination (rotarod), gait analysis, mechanical allodynia (VF), thermal hyperalgesia (hotplate, tail flick), grip strength
Intra-articular injections (Chemical models)		
MIA	Rat, mouse	Grip strength meter, thermal hyperalgesia, mechanical hyperalgesia, HL weight distribution (incapacitance), mechanical allodynia (VF), mechanosensitivity (EP), gait analysis (CatWalk), movement-induced nociception (Knee-Bend), movement and loading-induced nociception (CatWalk)
Na Urate	Cat, Parrot	Weight distribution, subjective pain scores
AIA	Mouse, Rat	HL weight distribution (incapacitance), mechanical allodynia (VF), 1ºmechanical hyperalgesia (PAM), 2º mechanical hyperalgesia (DPA), range of motion (VRA), gait analysis
Adjuvant	Rabbit, Rat	HL weight distribution; Mechanical hyperalgesia (VF)
Carrageenan/Kaolin	Mouse, Guinea pig, rat	Thermal hyperalgesia (Hargreaves & hotplate)
Collagenase (enzymatic)	Mouse, Rat (Adaes *et al.*, 2014; Adaes *et al.*, 2015)	Visual gait analysis (treadmill), joint tenderness (palpometer), movement-induced nociception (Knee-Bend), movement and loading-induced nociception (CatWalk)
Surgical		
ACLT	Rat, Dog, Rabbit	Gait analysis
MCLT	Rat	HL weight distribution (incapacitance)
MMT, MM (unilateral)	Rat, Sheep	HL weight distribution (incapacitance), mechanical allodynia (VF)
MM (bilateral)	Sheep	Ground reaction force
MM (partial)	Rabbit, Rat, Mouse	HL weight distribution(incapacitance), tactile allodynia (VF)
DMM	Mouse	HL weight distribution (incapacitance), mechanical allodynia (VF), thermal hyperalgesia, locomotor activity (LABORAS)
IA OC fragment	Horse	Clinical observation of lameness
ACLT& partial MM	Rat, Guinea pig	Gait analysis (CatWalk), mechanical allodynia (VF)
ACLT//MMT/MCLT	Rat	Rotarod
MCLT & MMT	Rat	Mechanical allodynia (VF), thermal hyperalgesia (Hargreaves apparatus), HL weight distribution (incapacitance), mechanical hyperalgesia (paw pressure device)

Table 1. Animal models used in the OA pain study. Adapted from Little & Zaki, 2012 and from Lampropoulou-Adamidou *et al,* 2014. Key: HL -hind limb, VF-Von frey filaments, EP - electrophysiological recordings from knee joint afferents, PAM-pressure application measurement device, ROM-range of motion analysis, VRA-videoradiographic analysis, DPA-dynamic plantar aesthesiometer (automated VF), LABORAS- laboratory animal behavior observation registration and analysis system, MIA-monoiodoacetate induced arthritis, ACLT-anterior cruciate ligament transection, MCLT- medial collateral ligament transection, MMT-medial meniscal transection, MM- medial meniscectomy, DMM- destabilization of the medial meniscus, IA OC fragment- intra-articular osteochondral fragment.

4.2 Collagenase model of Osteoarthritis

The collagenase-induced OA model belongs to the chemical induced models group and is based on joint-instability induction through intra-articular collagenase injection, being predominantly used to study mechanisms underlying structural joint damage (Blom *et al.*, 2004). Collagenase damages the structures that contain collagen type I, such as tendons and ligaments, leading to alterations of the joints. Histopathological alterations of the knee joint similar to those observed in human OA have been described after collagenase injection in rats (Al-Safar *et al.,* 2009; Adaes *et al.*, 2014) and mice (Blom *et al.*, 2004; Blom *et al.*, 2007), such as thinning of articular cartilage, cartilage matrix loss, loss of chondrocyte clustering, loss of proteoglycan staining and exposure of the subchondral bone (Adaes *et al.*, 2014). There are evidences that the temporal pattern of these changes directly correlates with the time of OA development elapsed following its induction by collagenase injection (Al-Safar et al., 2009; Adaes *et al.*, 2014).

Articular cartilage is not the only structure affected by collagenase; the subchondral bone and synovial membrane are also targets of modifications. Indeed, upon damage of the cartilage, the subchondral bone slowly becomes exposed to an harmful environment and an (almost) bone-to-bone friction leads to bone fissures that has also been described in the collagenase model (Adaes *et al.*, 2014). Moreover, a moderate inflammatory reaction was described in the mice (van der Kraan *et al.*, 1989) and rats' (Adaes *et al.*, 2014) knees in the initial phase of OA, as indicated by synovial infiltration with inflammatory cells and joint swelling, portraying the inflammatory response observed in OA humans. Thus, these modifications reproduce some of the main features associated with OA progression in humans.

These findings suggested that the intra-articular injection of collagenase is a promising alternative to study OA-associated pain. For that reason, our group recently investigated if the intra-articular collagenase injection in the rat knee could be a good model to study OA-associated nociception in rats. Thus, during 6 weeks, nociception induced by movement and loading on the affected joint was evaluated in the animals by the Knee-Bend and CatWalk tests. The results demonstrated significant differences between OA and control animals with an increase in the ipsi-contra ratio for the Knee-Bend score in OA animals, and a reduction in the ipsilateral paw print intensity of OA animals, until the sixth week. Therefore, for the first time, it was demonstrated that rats displaying OA structural features induced by collagenase injection in the

knee, also showed nociceptive behaviour associated with movement and loading on the OA joint, which represent patients´ major complaints (Adaes *et al.*, 2014).

5. Regeneration associated with osteoarthritis

5.1 Regeneration associated genes after PNI (peripheral nerve injury)

Neurons injured in the adult mammalian CNS normally fail to regenerate. In contrast, following injury to the PNS neurons reveal robust regenerative response (Harel & Strittmatter, 2006; Starkey *et al.*, 2009). However, the molecular mechanisms underlying successful nerve regeneration in the PNS remains to be clarified.

For the success of nerve regeneration is essential an intrinsic growth ability and an extrinsic permissive environment. The intrinsic growth refers to the ability of injured neurons to coordinate the expression of some genes that probably assist rapid regeneration, called regeneration-associated genes (RAGs) (Raivich & Makwana, 2007). This intrinsic growth depends on the existence of a permissive environment that is favorable for the axonal regrowth of surviving neurons. Schwann cells and macrophages are part of this environment and they are at the injury site to phagocyte the degenerative products. Beyond them, astrocytes and microglia complete this environment by surrounding the cell bodies (Leon *et al.*, 2000; Moran & Graeber, 2004). Once Schwann cells and macrophages are active in the injury site they synthesize a cocktail of neurotrophic factors such as nerve growth factor (NGF), brain-derived neurotrophic factor (BDNF) and neurotrophin-3 (NT-3), and cytokines. Consequently, begins the activation of an intrinsic growth program that includes the production of some proteins involved in regeneration. It is known that sensory neurons of the DRG are the most favorable neuronal population to address interactions between peripheral regenerative mechanisms and CNS growth and therefore, the expression of many RAGs has been studied in this population after situations of peripheral lesion (Snider *et al.*, 2002).

Activating transcription factor 3 (ATF-3) is, as previously stated, known as an injury marker in the nervous system, but, actually ATF-3 overexpression revealed pro-regenerative and neuroprotective functions not only improving regeneration of peripheral and central DRG branches but also causing neurite growth (Seijffers *et al.*, 2007; Fagoe *et al.*, 2015). Growth associated protein (GAP-43) is a regeneration-associated protein which was shown to be increased in DRG neurons after induction

of OA by MIA (Ferreira-Gomes *et al.*, 2012b), and is an important regulator of growth cone motility during nervous system development (Snider *et al.*, 2002). Small proline rich protein 1A (SPRR1A) was also associated to regeneration having been detected during successful sciatic nerve regeneration in the mouse. However, unlike GAP-43, SPRR1A is not expressed during development or in naïve adult tissue (Bonilla *et al.*, 2002). SRY-BOX11 transcription factor (SOX11) is expressed during the developing nervous system and it has been shown to have an important role in axon growth (Jankowski *et al.*, 2009). TRAF family member-associated NF-Kappa B activator (TANK) is another molecule that is increased in response to peripheral nerve injury and, furthermore, it has been reported that its expression is regulated by SOX11 (Salerno *et al.*, 2013). The brain-soluble protein BASP1 belongs to the family of growth-associated proteins, which also includes GAP-43, and is expressed in several tissues (Carpenter *et al.*, 2004), but more abundantly in neurons throughout brain development. BASP1 expression is increased during nerve regeneration and in adult neurons its overexpression promotes sprouting (Korshunova *et al.*, 2008). Although they belong to the same family, BASP1 appears later in development than GAP-43 (Console-Bram *et al.*, 1996).

Hereupon, our group hypothesized that the neuronal injury observed in DRG neurons innervating OA joints, indicated by the expression of ATF-3 and also NPY (Ferreira-Gomes *et al.*, 2012b), could induce a regeneration response reflected in an upregulation of some of these molecules. In fact, the increased expression of one of these molecules, GAP-43, had already been shown by our group in DRG neurons of MIA-induced OA rats (Ferreira-Gomes *et al.*, 2012b), as already mentioned. Thus, in the collagenase model, the expression of some RAGs, including SPRR1A, SOX11, TANK and BASP1, was evaluated in sensory neurons innervating OA joints. It was found by RT-PCR analysis that *Sox11* and *Sprr1a* mRNA expression was induced during OA in DRG neurons, while *Tank* and *Basp1* levels remained unaffected. Nonetheless, the most marked changes were observed in the expression of the *Sprr1a* gene. Western Blot analysis confirmed the previous result showing an increased expression of SPRR1A in the ipsilateral DRG of collagenase injected rats. Through immunohistochemical experiments, our group evaluated as well the cellular localization of the SPRR1A protein. Data in the DRG of OA rats was consistent with a pattern of SPRR1A staining in neuronal cell bodies and axonal processes. In addition, double immunolabelling for SPRR1A and ATF-3 showed a higher

percentage of co-localization in OA animals comparing with the control animals, suggesting that during OA SPRR1A is preferentially expressed in injured neurons. These results may indicate that the regenerative process associated with lesion of nerve terminals may play a role in nociception associated with OA (Adães *et al*., unpublished data).

5.2 Small proline rich protein 1A (SPRR1A)

The human SPRR genes consist of two SPRR1 genes (SPRR1A and 1B), seven SPRR2 genes (SPRR2A, 2B, 2C, 2D, 2E, 2F and 2G) and a single SPRR3 gene. All three members encode small proteins that are rich in proline and are built up from repeating elements (Gibbs *et al.*, 1993). In 1988, the proteins belonging to this class were identified for the first time as major components of the cross-linked cornified envelop of skin keratinocytes and from this moment, the multigene SPRR family became part of the keratinocyte differentiation markers (Kartasova *et al.*, 1988). A few years later, SPRR1A was proposed as a new regeneration associated gene since it was highly expressed in DRG neurons after peripheral nerve injury and during sciatic nerve regeneration (Bonilla *et al.*, 2002; Jankowski *et al.*, 2009). Thus, it seems that SPRR1A induction is related with a regenerative capacity, being highly expressed in the cell bodies and central terminals of primary sensory neurons following peripheral nerve injury. However, at the time, a detailed characterization of SPRR1A expression had not been made, and it was extremely important to realize which DRG subpopulations express SPRR1A. Co-expression of SPRR1A with specific DRG subpopulations markers showed that there is a co-localization of SPRR1A with CGRP, IB4 and NF200, revealing that all three subpopulations express SPRR1A (Starkey *et al.*, 2009).

A possible mechanism of SPRR1A expression involves the RAG *Sox11*. SOX11 proteins have an important role in cell fate, survival and differentiation across all developing organ systems (Lefebvre *et al.*, 2007) and their dysfunction probably is related with several diseases. The expression of this molecule in DRG increased the axonal growth rate after crush injury; however, SPRR1A seems to be indispensable for the effect of SOX11, since SPRR1A knockdown significantly reduced the stimulatory effect of SOX11 on neurite outgrowth. On the other hand, the SOX11 expression in DRG neurons driven by the herpes simplex virus conjugated with the *Sox11* gene (HSV-SOX11) caused a significant increase in SPRR1A expression.

These data suggest that the transcriptional activation of SPRR1A by SOX11 is a critical step in nerve regeneration (Jing *et al.*, 2012). Results obtained by our group go in line with this, since after OA induction there was an increase of both genes (Adães *et al*., unpublished data). Additionally, there seems to be an interaction between ATF-3 and SOX11 because ATF-3 expression was reduced in response to SOX11 knockdown (Jankowski *et al.*, 2009). Curiously, the inverse was not found, i.e., ATF-3 knockdown had no effect on SOX11 level (Jankowski *et al.*, 2009). This suggests that SOX11 may influence the regulation of ATF-3 gene expression. As above mentioned, our group observed very high levels of co-expression of SPRR1A and ATF-3 in the collagenase OA model which suggest that SOX11, ATF-3 and SPRR1A are probably part of the same regeneration-inducing signaling pathway (Adães *et al*., unpublished data). Thus, it is possible that SOX11 is upregulated in response to injury of sensory nerve endings associated with OA, which may induce the expression of ATF-3 and SPRR1A, among other RAGs, to initiate the regenerative process.

6. An approach to gene delivery

6.1 Adeno-associated virus (AAV) as vectors

Vector choice plays a crucial role for the success of gene therapy and several considerations must be taken into account, like the capacity to attach to and enter the target cell, to be successfully transferred to the nucleus, the ability to be expressed in the nucleus for a continued period of time and the lack of toxicity (Daya & Berns, 2008). Presently, the most successful gene therapy strategies are related to recombinant viral vectors (e.g., adeno-associated virus, adenovirus, lentivirus, retrovirus, and herpes simplex virus) (Yu *et al.*, 2016). Adeno-associated virus (AAV) has been one of the most widely used vector systems for gene therapy because of its lack of pathogenicity, its persistence, its low immunogenicity, the existence of several serotypes and its broad cellular tropism (Daya & Berns, 2008). AAV is a non-enveloped parvovirus that requires the presence of a helper virus for efficient replication (Buller *et al.*, 1981). The wild-type AAV genome consists of a linear single-stranded DNA molecule with approximately 4.7 kilobases that includes two open reading frames, Rep and Cap, flanked by inverted terminals repeats (ITRs)(Koczot *et al.*, 1973). ITRs are necessary for replication and packaging so, for gene delivery the transgene is placed between the two ITRs, and Rep and Cap are supplied in trans. Following molecular transduction of target cells the rAAV

(recombinant adeno-associated virus) genome must be converted to double-stranded transcriptionally active forms to facilitate transgene expression (Weitzman & Linden, 2011).

Several serotypes of AAV vectors have been identified and they are used to direct transgene expression in a variety of tissues, including the nervous system, but most studies for gene therapy are based on the AAV serotype 2. The AAV2 vector genome can be crossed-packaged with capsids from different AAV serotypes resulting in increased neural tropism and spread of the viral transgene (Rabinowitz *et al.*, 2002).

6.2 Intra-ganglionic injection - DRG as a target for gene delivery

Several studies have shown that gene therapy targeting the PNS can be an approach for chronic pain treatment (Handy *et al.*, 2011; Goins *et al.*, 2012). It is known that after a peripheral injury several cellular mechanisms are altered and this disturbance resides in diverse sites, including in the soma of the injured sensory neurons. DRG contain the cell bodies of these neurons and therefore are an ideal target for therapeutic gene transfer (Yu *et al.*, 2016). Accordingly, gene transfer to sensory neurons within the nociceptive pathway is a new tool to study pain. Lately, the rAAV vector system has received a sudden attention for *in vivo* viral gene transfer to the DRG neurons in various animal models of chronic pain. For example, intra-ganglionic injection of AAV2/8 carrying the recombinant gene for serine protease inhibitor 3 attenuated neuropathic pain after spared nerve injury (Vicuna *et al.*, 2015). In another study, similar results were obtained after intra-ganglionic injection of an AAV2/5 carrying a gene for short hairpin RNA targeting the $Na_v1.3$ channel (Samad *et al.*, 2013). Recently, the AAV2/5 serotype showed an efficient transduction rate in DRG neurons, including small peptidergic neurons and small non-peptidergic neurons (Mason *et al.*, 2010).

Another type of approaches can be done in order to target the DRG. Thus, intrathecal delivery of AAV produces effective gene transfer to the DRG and spinal cord (Federici *et al.*, 2012; Fagoe *et al.*, 2014); however, this type of methodology requires far more AAV vector, making it a more expensive method compared to the intra-ganglionic injection (Fagoe *et al.*, 2014). Furthermore, due to propagation of the vectors into the cerebrospinal fluid (CSF) there is also a robust transduction in several spinal cord tissues including spinal motor neurons (Federici *et al.*, 2012). Thus, AAV

intrathecal administration may be more effective in neurological disease processes that require gene delivery to motor neurons (Federici *et al.*, 2012). Intraneural injections into the sciatic nerve are another route of AAV delivery, but despite it can transfer genes to primary sensory neurons, the transduction of motor neurons is preponderant (Boulis *et al.*, 2003). Intramuscular AAV injection does not show efficiency in transducing sensory neurons (Towne *et al.*, 2009), unlike intraperitoneal AAV injections (Machida *et al.*, 2013).

Objectives

Acknowledging our previous results where an upregulation of SPRR1A was observed after OA induction by intra-articular collagenase injection, we aimed at better understanding the SPRR1A role in this pathology, as well as its potential role as a treatment target, by upregulating its expression in DRGs, through gene delivery, and evaluating its effects on the nociceptive behavior. For that purpose, the following objectives were pursued:

- To ascertain the efficiency of the intra-ganglionic AAV injection – To achieve this goal we performed the intra-ganglionic injection of a recombinant adeno-associated virus (rAAV) engineered to express green fluorescent protein (GFP) as a reporter gene, in DRG of naïve rats. To assure the best efficiency, different end-points of viral transduction were studied (4, 6 and 8 weeks after intra-ganglionic surgery), by using immunohistochemistry against GFP to quantify the percentage of sensory neurons expressing GFP.
- To evaluate which type of cells are transfected by the AAV - By double immunohistochemistry we analyzed the co-localization between GFP and GFAP (a marker of Satellite glial cells) in DRGs neurons from naïve animals injected with AAV-GFP.
- To evaluate the effect of SPRR1A overexpression on the nociceptive behavior of controls and OA animals – To achieve this, the intra-ganglionic injection of either rAAV-GFP or rAAV-SPRR1A was performed in both OA and control animals and their nociceptive behavior was evaluated by using the CatWalk, Von Frey, Knee-Bend and Rota-rod tests. An additional group of control and OA animals received an intra-ganglionic injection of saline.
- To evaluate SPRR1A expression in control and OA animals injected with rAAV-GFP, rAAV-SPRR1A or saline – To achieve this, the SPRR1A gene expression was evaluated in DRGs by real-time quantitative PCR.
- To evaluate expression of other markers of neuronal damage/ regeneration in OA and control animals injected with rAAV-SPRR1A- In order to achieve this goal, the expression of ATF-3 was quantified in DRGs by real-time quantitative PCR, as well as that of GFAP, considered a marker of SGCs

increased activation.

- To evaluate the extent of the histopathological lesions of knee joint sections - By staining knee sections by the Fast Green and Safranin O histological method, the pathological changes in the knee joints of OA animals following intra-ganglionic injections of AAV-SPRR1A, AAV-GFP or saline were assessed.

Materials and Methods

1. Animal Handling

Experiments were carried out in adult male Wistar rats weighting between 175 and 225g at the beginning of the investigation. The 43 rats used were housed in Biotério Geral do Centro de Investigação Médica da Faculdade de Medicina da Universidade do Porto, two per cage with water and food ad *libitum*, under controlled conditions of temperature and humidity, 22±2ºC and 55±5%, respectively. In addition, the lighting conditions were also controlled (12-hour light/12-hour dark cycle).

Of all the animals used in this research, 14 were from Biotério Geral do Centro de Investigação Médica da Faculdade de Medicina da Universidade do Porto, while the remaining 29 animals were from Charles River (France). Animals from Charles River required a period of adaptation to the animal facility conditions of 5 days. After this period, all the animals went through a phase of 4 days of habituation to manipulation by the researcher as well as to the behavioural nociceptive tests. During all the period of the research procedures, the health state of the animals was ascertained, with particular attention to weight loss, loss of mobility, bad healing, opening of stitches and self-mutilation.

All the experimental procedures were performed according to the ethical norms for the study of experimental pain in conscious animals (Zimmermann, 1983), as well as the regulations of local authorities on the use of animals for scientific purposes.

2. Induction of osteoarthritis - Intra-articular injection of Collagenase

To induce osteoarthritis in the animals, an intra-articular injection of 500 U of type II collagenase (ColII, Sigma-aldrich, St. Louis- USA) was performed under a brief isoflurane anaesthesia (5% for induction, 2.5% for maintenance). Intra-articular injections were performed using a Hamilton syringe with a 26 G needle inserted through the patellar ligament into the right knee joint cavity. Animals received two injections, separated by three days, of 25 µL of either saline (control group) or 500U of ColII from Clostridium histolyticum dissolved in saline and filtered thought a 0.22 µm membrane (OA group), as previously described (Adaes *et al.*, 2014).

3. Construction of viral vectors

Viral vectors containing humanized GFP and SPRR1A were a gift from Jack Kanaan and Nick Lipton from the University of Michigan, USA. Briefly, GFP and SPRR1A genes were inserted into an adeno-associated virus plasmid backbone. Expression of the transgenes was driven by the chicken beta actin/cytomegalovirus enhancer (CβA/CMV) promoter hybrid. The vectors contained AAV2 inverted terminal repeats (ITRs) and were packaged into AAV5 capsids via co-transfection with a plasmid containing *rep* and *cap* genes and adenovirus helper functions. Thus, two adeno-associated virus constructed in the same way served as vectors to GFP (AAV2/5-GFP) and SPRR1A (AAV2/5-SPRR1A) (Polinski *et al.*, 2015). The vectors titer used in this study was $5.88x10^{13}$ genomes/mL. With the aim of preserve the viral stability and titer, viral preparations were stored at 4ºC. Additionally, syringes, pipettes and microcentrifuge tubes which contacted the viruses were first coated in SigmaCote ® (Sigma-Aldrich, St. Louis, USA) to minimize binding of viral particles (Polinski *et al.*, 2015).

4. Intra-ganglionic injections of rAAV 2/5-SPRR1A, rAAV2/5-GFP and saline

Fourteen days after intra-articular injections of ColII or saline, animals were submitted to an intra-ganglionic injection of rAAV2/5-SPRR1A, rAAV2/5-GFP or saline. After intraperitoneal anaesthesia with Medetomidine hydrochloride (0.5mg/kg, Domitor ®, Esteve Farma, Carnaxide-Portugal) and ketamine hydrochloride (75mg/kg, Imalgene ®, Merial, Lyon-France) diluted in distilled water, the back of the animals was shaved in order to put the area of interest more visible and cleaner. Subsequently, animals were placed in a stereotaxic frame and a small incision was made in the skin just to the right of the dorsal midline starting from the superior iliac crest. Then, the superficial muscular fascia was incised and the paraspinal muscles were separated by a combination of several lateral cuts until the right transverse processes of the lumbar vertebrae (L5 and L4) were achieved. Exposure was maintained using a surgery retractor and while using binocular magnification, the L4 and L5 transverse processes were broken with a rongeur to access beneath them the L4 and L5 ganglia, which comprise the cell bodies of the sensory neurons that innervate the knee joint. The muscle and bone removal was minimised only to the enough to perform the intra-ganglionic injection.

A Hamilton syringe fitted with a glass capillary needle (coated with SigmaCote ®) was used for the injection and the tip of all glass capillaries used was pulled to a small diameter to maintain the rigidity to penetrate DRG, with minimum damage. The Hamilton syringe was fixed to the stereotaxic frame (90º from horizontal) in order to move it downwards to allow the glass capillary needle to reach the DRGs. When the glass capillary needle was inside each DRG the syringe was slowly pushed to inject 3 μL of rAAV-SPRR1A, rAAV-GFP or saline. Posteriorly, the glass capillary needle was slowly withdrawn.

At the end of this procedure the wound was closed in layers (muscle and skin) using surgical sutures (4-0 Sutura cirúrgica de seda, Silkam). The intervened area was disinfected with Betadine ® (Meda Farma, Lisboa-Potugal) and all animals were rehydrated with a subcutaneous injection of 2 mL of 0.9 % saline (Braun, Queluz de Baixo-Portugal). The sedative effect of the anesthesia was reverted by an intramuscular injection of 0.02 mL/100 g of atipamezole hydrochloride (1 mg/kg; Antisedan ®, Esteve Farma, Carnaxide- Portugal). About half an hour after the reversal of the sedative effect, 0.1 mL of tramadol (Tramal **®,** Grünenthal, Amadora-Portugal) was orally administered to alleviate post-surgical pain.

5. Behavioural Testing

The animals were accustomed to each of the behavioural tests used in this study for a minimum period of at least 4 days. Behavioural tests were performed in all animals in the same order (namely, 1st CatWalk, 2nd Von Frey, 3rd Knee-Bend and 4th Rotarod) and at the following time points: 1) Before OA induction or saline injection (at day 0); 2) Before intra-ganglionic injections of AAV-GFP/AAV-SPRR1A/saline (at days 7 and 14 after collagenase or saline knee injection); 3) After the intra-ganglionic surgical procedure (at days 21, 28, 35 and 42 after collagenase or saline knee injection), as depicted in Fig. 5. The behavioural analyses of AAV2/5-SPRR1A animals are relative to 20 animals (control n=10 and OA n=10). Regarding the AAV-GFP animals, the behavioural analyses correspond to 10 animals (control n=5 and OA N=5), while the saline group comprises 4 animals (control n=2 and OA n=2).

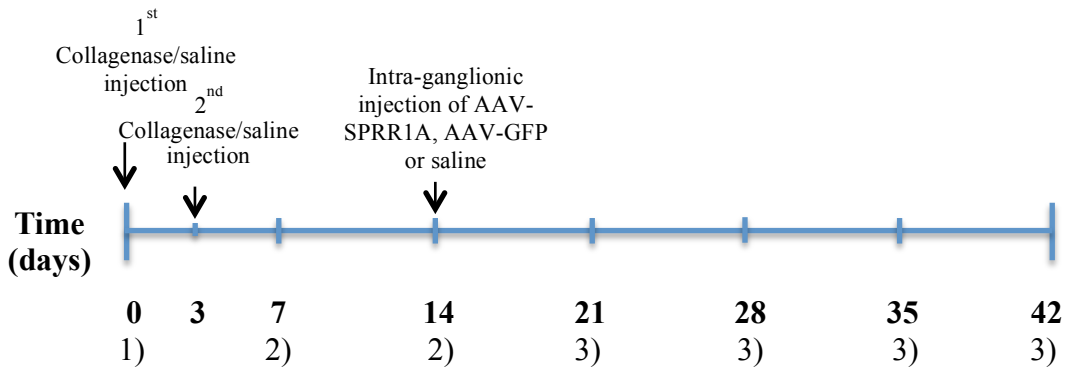

Figure 5. Timeline for behavioural analyses.

5.1 CatWalk test- Assessment of movement-evoked pain

The CatWalk test consisted in placing the animals in a glass platform equipped with a light from LEDs located in a dark compartment. Animals were allowed to walk freely and a bright image, only at the points of contact of the paw with the surface, was produced. Under the glass platform, a video camera that was connected to a computer equipped with video acquisition software (Ulead Video Studio, Freemont, CA) monitored the animals` movements. The signal intensity depended on the area of the paw in contact with the platform and increased with the pressure applied by the paw. From the recorded videos, random frames were analysed: three pairs of frames (one for each hind paw) with the animal walking and three frames with the animal standing still. The number and intensity of pixels above a defined threshold were quantified, for each hind paw. This analysis was made with Image J software in order to determine the total hindpaw print intensity (mean pixel intensity x number of pixels). Results were expressed as the percentage of the total ipsilateral hindpaw print intensity (%TIPPI) in the total intensity of both hindpaw prints (Ferreira-Gomes *et al.*, 2008).

5.2 Von Frey test- Assessment of mechanical allodynia

In the Von Frey test, animals were placed in a grid with small holes. The meshed grid allowed the application of the Von Frey filaments to the central region of the plantar surface of the animals´ hind paws. This stimulation was made in ascending order of force using the Touch Test Sensory Evaluator Kit (Stoelting, Wood Dale, USA)- 0.008g; 0.02g; 0.04g; 0.07g; 0.16g; 0.4g; 0.6g; 1.0g; 1.4; 2.0g; 4.0g; 6.0g; 8.0g; 10.0g; 15.0g; 26.0; 60.0g; 100.0g; 180g; 300g. It was considered an escape response caused by pain when animals abruptly shacked the hindpaw and when they

licked it. The lowest value of force required to elicit a positive response was considered to be the paw withdrawal threshold (PWT). However, for each test 3 trials were performed, with a break of 2 minutes between each. The up-down method was the one used, i.e. in the absence of a paw withdrawal response to the selected hair, a stronger stimulus was presented, in the event of paw withdraw, the next weaker stimulus was chosen, as previously described (Bonin *et al.*, 2014).

5.3 Knee-Bend test-Assessment of movement-evoked pain

The Knee-Bend test consisted in counting the number of squeaks and/or struggle reactions of the animals in response to alternate flexions and extensions of the knee joint. Both hind paws were evaluated and each test included 5 flexions and 5 extensions. The score of the test was determined according to the type of reaction: Score 0 was given when there was no response to any kind of movement (flexion and extension); score 0.5 when there was struggle reaction in response to maximal flexion/extension; score 1 when there was struggle reaction in response to moderate flexion/extension and also when there were vocalizations in response to maximal flexion/extension and score 2 was given to squeak reactions in response to moderate movements (flexions and extensions) of the joint. The sum of the registered reactions, giving maximal values of 20, represents the Knee-Bend scores, an indication of the animal´s nociception. The contralateral knee was always evaluated first, in order to avoid an increase in the contralateral score arising from the manipulation of the injected knee (Ferreira-Gomes *et al.*, 2008).

5.4 Rotarod test- Assessment of motor coordination

The Rotarod test has been used to evaluate the motor coordination of the rats. This test consisted in placing the animals on a horizontal rod that rotates about its long axis and the time that the animals stayed without falling was recorded. The apparatus is configured to accelerate from 4 to 40 rpm in 300s, however, during the period of habituation the animals stayed in the apparatus at a constant speed of 4 rpm (Piel *et al.*, 2014).

6. Tissue Preparation

Naïve animals with rAAV-GFP injection were perfused at three different time points (4, 6 and 8 weeks after intra-ganglionic injection, n=3 for each time point) for later immunohistochemical analysis. OA and control animals with rAAV-SPRR1A (n=10, 5 OA and 5 control), rAAV-GFP (n=4, 2 OA and 2 control) and saline injections (n=4, 2 OA and 2 control) were euthanized by decapitation 6 weeks after model induction for gene expression studies.

6.1 Tissue processing for Immunohistochemistry

For the immunohistochemistry group, animals were intraperitoneally anesthetized with sodium pentobarbital (100 mg/kg, Eutasil ®, Ceva, Algés-Portugal) diluted in 0.9% saline and then perfused. The perfusion consisted in opening the abdominal and thoracic cavities in order to expose the heart. When exposed, 0.1 mL of heparin was injected into the left ventricle and a cannula was inserted in the aorta through an incision in the same ventricle. Thereby, about 300 mL of oxygenated Tyrode`s solution (wash solution) circulated followed by 800 mL of a fixative solution containing 4% paraformaldehyde (PFA) diluted in phosphate buffer saline 0.1M (PBS 0.1 M). At the end of the perfusion the animals were dissected and L3, L4 and L5 spinal cord segments were collected along with their roots and DRGs. The collected material was post-fixed for 4 hours in the same fixative solution and then kept in 30% sucrose with 0.01% sodium azide, until they were processed.

DRGs were serially sliced in 12µm thick sections, using a cryostat (Leica instruments GmbH, CM3050, Germany), and collected into poly-L-Lysine coated slides. Each DRG was collected in 6 sequential series, with an average of 12 sections per slide. After cutting, the slides were dried on a heating plate for 1 hour at 37ºC and thereafter were stored at -20ºC until use in immunohistochemical reactions.

6.1.1 Immunoreaction against GFP

The slides containing the L4 and L5 DRG slices of naïve animals intra-ganglionically injected with rAAV-GFP sacrificed at different time points (4, 6 and 8 weeks after surgery) were thawed and washed firstly in PBS 0.1M and then in PBST. Then, sections were incubated with the blocking solution (10% Normal goat serum, NGS, diluted in PBST) to avert unspecific ligations. After, the sections were

incubated overnight in the primary antibody against GFP (polyclonal rabbit anti-GFP; 1:1000, Abcam, USA) diluted in PBST containing 2% NGS. In the next day, the sections were washed in 2% NGS in PBST and incubated in the dark in the secondary antibody (Alexa 594 goat anti-rabbit; 1:1000; A11012 Life Technologies, Eugene, USA) diluted in PBST containing 2% NGS. From this moment on the slides were always protected from light, being washed in PBST followed by PBS and stored in PBS 0.1M at 4ºC until visualization under the fluorescent microscope. At the time of microscopic analysis, the slides were coverslipped with a glycerol solution prepared with PBS 0.4M. Microscopic analysis was performed by using a fluorescent microscope (AXIO Imager.Z1, Zeiss, Germany) coupled to a digital camera (Axiocam MRm, Zeiss, Germany) and an image software (Axiovision 4.8 software, Carl Zeiss MicroImaging) to capture the images. The total number of cells was counted as well as the number of GFP labelled cells. This was performed with the aid of Image J ® computer program. Data is presented as the percentage of cells expressing GFP in L4 and L5 DRG.

6.1.2 Double immunoreaction against GFP and GFAP

In order to analyze if the rAAV transfected not only neurons, but also satellite glial cells, a colocalization of GFP with GFAP was performed. This double reaction was made in slides containing the L4 and L5 DRG slices of naïve animals intra-ganglionically injected with rAAV-GFP. L4 and L5 slices were thawed and washed in PBS 0.1M and PBST. After this, sections were incubated with blocking solution (10% NGS in PBST) and then immunoreacted against GFP (rabbit anti-GFP; 1:1000, Abcam, USA) and GFAP (mouse anti-GFAP; 1:1000, Cell Signaling, Netherlands) during 24h. Sections were then washed in 2% NGS diluted in PBST and incubated in the dark with secondary antibodies (Alexa 488 donkey-anti-mouse; 1:1000; A21202 Molecular Probes, Eugene, USA and Alexa 594 goat-anti-rabbit; 1:1000; A11012 Life Technologies, Eugene, USA) diluted in PBST containing 2% of NGS. Lastly, sections were washed in PBST followed by PBS and stored in PBS 0.1M at 4ºC until visualization under the fluorescent microscope. At the time of microscopic analysis, the slides were coverslipped with glycerol prepared with PBS 0.4M.

6.2 Tissue processing for real time quantitative polymerase chain reaction (real time qPCR)

For the gene expression studies the animals were euthanized by decapitation after being slightly sedated with isoflurane. Their L3-L5 ipsilateral and contralateral DRGs as well as their corresponding spinal cord segments were fleshly harvested into RNase free eppendorfs, immediately put on ice and preserved at -80ºC until further use. The L4 and L5 DRGs, of each side, were pooled together.

6.2.1 RNA extraction

Total RNA was extracted using the RNAqueous-MicroTotal isolation Kit (Ambion). Briefly, 100 mL of lysis buffer was added to the samples, and they were homogenized using magnetic beads and centrifuged at 21000 g for 5 min. The cleared supernatant was transferred to a new RNase-free tube and the half volume of 100% ultra pure ethanol was added. Samples were briefly vortexed and then transferred to a micro filter cartridge. After, samples were centrifuged at 12000 g for a few seconds in order filter the protein from the RNA. Afterwards, the protein was discarded and a new collection tube was applied to the micro filter cartridge. The samples were washed with 180 μL of wash solution 1 (provided with Ambion isolation Kit) and centrifuged during a few seconds. Then, samples were washed with 180 μL of wash solution 2/3 (provided with Ambion isolation Kit) followed by centrifugation during a few seconds. This wash was repeated once. After dumping the collector tube, the micro filter cartridge was replaced into the same collection tube and centrifuged during 2 min to remove residual fluid and dry the filter. Finally, the micro filter cartridge was transferred to a micro elution tube (1.5 ml tubes provided with the kit) and 10μL of the elution solution, preheated to 75ºC, was added. A centrifugation was made for a few seconds and RNA was eluted from the filter. This elution step was repeated with a second 7μL aliquot of elution solution, collecting the eluate in the same micro elution tube. The micro filter cartridges were discarded and the micro elution tubes were stored. RNA was quantified by NanoDrop 2000 (Thermo Scientific NanoDrop 2000 spectrophotometer) and its integrity was assessed (absorbance 260/280 and 260/230 ratios).

6.2.2 cDNA synthesis

1,5 μg of total RNA was reversed transcribed using the Tetro cDNA synthesis kit (Bioline, A meridian Life Science ®, USA) and random primers. In each reaction 1μL of Oligo(dt)$_{18}$ primer, 1μL of 10 nM dNTP mix, 4μL of RT buffer, 1μL of Rnase inhibitor and 1μL of Tetro reverse transcriptase were added to a total mix of 12μL of water and RNA (12-V_{RNA} = $V_{MilliQ\ water.}$). Samples were incubated at 45ºC for 50 min followed by 85ºC for 3 min in a Biorad T100 Thermal Cycler. The resulting cDNA was diluted 1:3 and stored at -20ºC for later use.

6.2.3 Real-time qPCR

Relative gene expression levels were measured by real-time qPCR using the StepOnePlus Real-time PCR system (Applied Biosystems). The PCR mix was prepared by adding 7μL of SYBR ® Select Master Mix (Applied Biosystems), 1μL of the primer mix, 5μL of MilliQ water and 1μL of cDNA sample for a final volume of 14μL. Each PCR mix was prepared in triplicate. Primer sequences are listed in Table 2. The reaction plate was sealed, centrifuged briefly and placed in the Real-Time PCR system. The amplification protocol consisted in forty cycles with denaturation at 95ºC for 15s, followed by annealing at 60ºC for 30s and extension at 72ºC for 30s. Target gene expression was normalized against to the expression of the endogenous glyceraldehyde-3-phosphate dehydrogenase (*Gadph*).

Transcript	Primers sequences
SPRR1A	F: GAGCCTGCTCTTCTCTGAGTATT R: TGAGGGGGTACAGTGCAAGG
ATF-3	F: CCAGAACAAGCACCTTTGCC R: GTTTCGACACTTGGCAGCAG
GFAP	F: AATTGCTGGAGGGCGAAGA R:TTGAGGTGGCCTTCTGACAC
GAPDH	F: CCATCACCATCTTCCAGGAG R: GCATGGACTGTGGTCATGAG

Table 2. Primers sequences for real-time qPCR; F: forward primer; R: reverse primer

7. Histological analysis of the knee joints

The use of calcified bone samples allows the bone mineral phase to be intact. Methylmethacrylate has been widely used as an ideal medium to soak calcified bone because of its hardness (Dominguez *et al.,* 2012). The knee joints of the control and OA animals that were used to study gene expression were dissected and immersed in 70% alcohol in glass vials during three days, with daily change. In the next three days, the knees were immersed in 100% alcohol, with daily change. This dehydration was performed to promote the removal of water from the tissue and to allow subsequent infiltration of the resin. The next step was the diaphanization for total waste elimination and to allow the best favourable tissue conditions for resin infiltration. Thus, knees were immersed in a xylene solution during 8-12 hours. Infiltration is the time required for the methyl methacrylate resin (MMA) to dissipate throughout the sample by filling the tissue. This infiltration consists of phases A and B, and inclusion is made in a phase C. The solution of phase A is constituted by 75% of MMA (Merck ®, $C_5H_8O_2$, Darmstadt- Germany) and 25% of Dibutylphthalate 99% (DF) (Sigma-Aldrich ®, $C_{16}H_{22}O_4$, St. Louis- USA). The knees remained in this solution for three days at 4ºC, with daily change. In a next phase solution A was replaced by a solution B with 75% of MMA, 25 % of DF and 1g of Benzoyl peroxide (BP) (Merck ®, $C_{14}H_{10}O_4$, Darmstadt- Germany), remaining three days at 4ºC with daily change. The last phase (C) was the inclusion in a solution comprising 75% of MMA, 25% of DF and 2.5g of BP. This solution was daily changed and on the third day the glass vials with the knees and with inclusion solution were placed in the oven at 37 ºC until polymerization. After polymerization of the resin, the glass vials that served as a template for inclusion were carefully broken allowing the microtomy of the block. The microtomy was done using an automatic microtome (Leica, RM 2255) with a tungsten blade and the blocks were cut into 5 μm sections into glass slides, and allowed to adhere to the slides in an oven during 24h.

Knee joint sections were stained by the Fast Green and Safranin-O method to evaluate the extent of the histopathological lesions, as previously described (Ferreira-Gomes *et al.*, 2012). Briefly, the staining protocol consisted in keeping the slides with the knee joint sections during 15 minutes in a 0.02% Fast Green solution, followed by a brief incubation of 30s in acetic acid. Then, the slides were maintained during 5 minutes in 0.5 % Safranin. Finally, the slides were washed in distilled water and kept

in the oven overnight to dry. After drying, slides were mounted with Entellan® (Merck, Darmstadt-Germany) and images were acquired with an Axioskop-40 microscope equipped with a Camera (Leica EC3 Microsystems, Switzerland).

Safranin O staining is directly proportional to the concentration of proteoglycan in the cartilage and the acidic Fast Green can bind to the collagen fibres in the subchondral bone. Therefore, this type of staining is a good approach to reveal the pathological changes in the knee joints (Ferreira-Gomes *et al.*, 2012).

8. Statistical Analysis

Statistical analyses were performed using the GraphPad Prism Software Version 6.0 for Macintosh. Results were presented as the mean ± SEM. For the number of GFP expressing cells (immunohistochemistry reactions) an unpaired t-test was performed to investigate differences on GFP expression in DRGs with different times of AAV transduction. Behavioral data was analyzed by a two-way analysis of variance (ANOVA) followed by the Bonferroni post-hoc test for comparisons between control and OA groups, between ipsilateral and contralateral sides and also between ipsilateral sides from different groups at each time-point. For comparisons within the same group repeated measures followed by Bonferroni post-hoc test was used. Gene expression data were analyzed by one-way ANOVA. In all statistically analysis the level of significance was considered as $p<0.05$.

Results

1. Evaluation of AAV2/5 transfection efficiency

In order to evaluate the best time for an efficient AAV2/5 transfection, DRGs of naïve animals with different times of AAV2/5-GFP transfection (4, 6 and 8 weeks after intra-ganglionic injection) were immunolabelled against GFP. Immunofluorescence results showed no significant differences in the transduction efficiency between the three time-points studied (Fig. 6C). Therefore, the 4 weeks of transduction was chosen for the remaining studies.

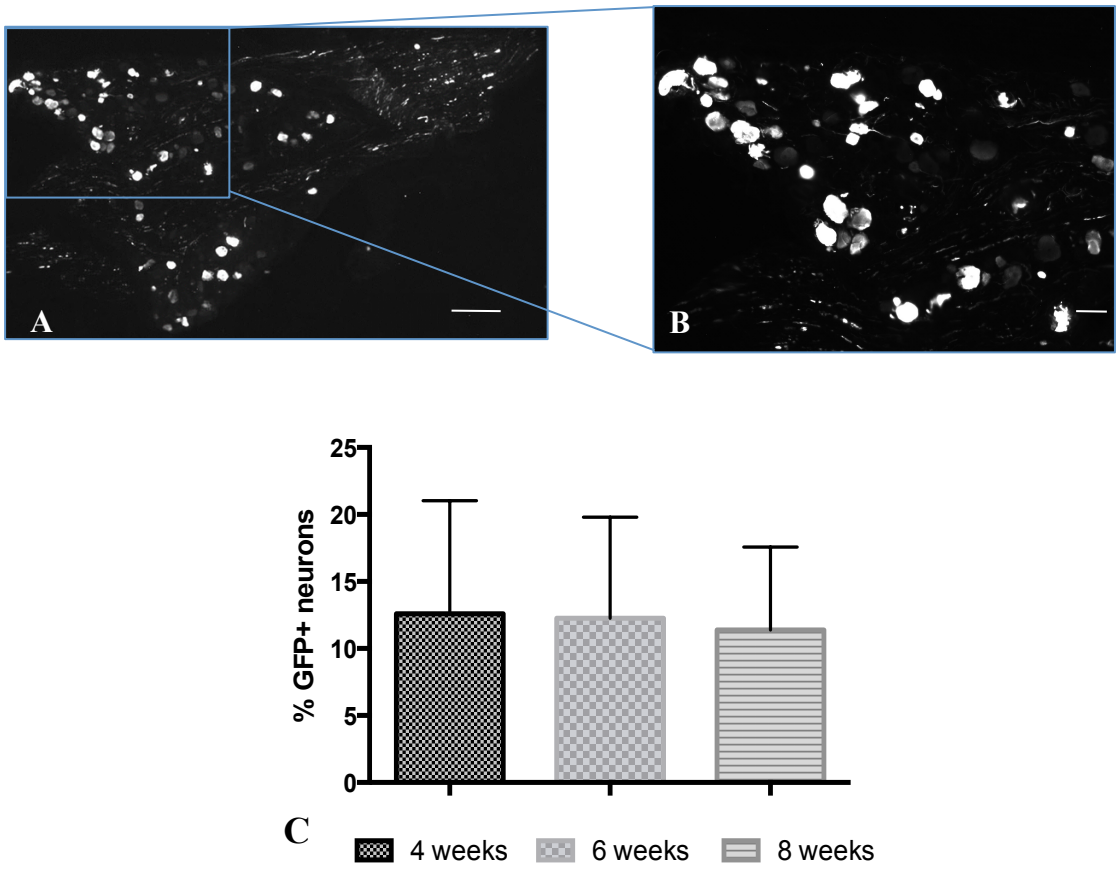

Figure 6. GFP expression in the DRG. **A, B-** Fluorescent microscope photos images depicting the neuronal populations transduced by AAV-GFP during 4 weeks. A- 2,5x magnification, scale bar represents 200 μm; B- 10x magnification, scale bar represents 50 μm. **C-** Immunofluorescence analysis of GFP expression in L4 and L5 DRGs injected with AAV2/5-GFP, and collected at different time points (4, 6 and 8 weeks after intra-ganglionic injection) Results are presented as the percentage of GFP labelled neurons in L4 and L5 DRG. Mean ± SEM. Unpaired t-test. No significant differences were found between the three time points evaluated.

2. Determination of AAV2/5 transfection in Satellite glial cells (SGC)

To investigate if, beyond neurons, AAV2/5 also transfects SGCs, ipsilateral L4 and L5 DRGs of naïve animals receiving an AAV-GFP intra-ganglionic injection were immunoreacted against GFP and GFAP (marker of activated satellite glial cells). No colocalization between GFP and GFAP was detected in our DRG samples, ruling out the possible transfection of SGC by AAV2/5 (Fig. 7).

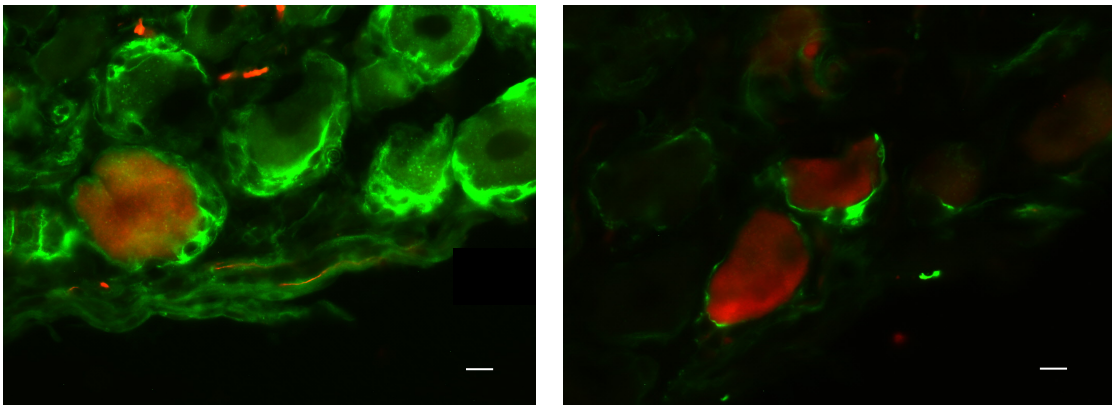

Figure 7. Double immunoreaction against GFP and GFAP. Fluorescent microscope photo images depicting a double immunoreaction against GFP (red, labelling the neuronal cell bodies) and GFAP (green, labelling the surrounding SGCs) in a L4 DRG with 4 weeks of AAV2/5-GFP transfection. No co-localization was observed. Scale bar represents 10 μm (40x magnification).

3. Evaluation of the animals´ behaviour following intra-ganglionic injection of AAV-GFP or of saline

After ascertaining that the best time for an efficient transfection of the AAV2/5 was 4 weeks, intra-articular injections of saline (control animals) and collagenase (OA animals) were performed in the right knee of a new animal group. After 14 days animals were intra-ganglionically injected with AAV2/5-GFP or saline. The AAV-GFP group was used as control of AAV-SPRR1A injections and the saline group as a control of the intra-ganglionic injection. The nociceptive behaviour of the animals was evaluated, during 4 weeks, by the CatWalk and the Knee-Bend tests, which assess movement- and loading-evoked pain, as well by the Von-Frey test that evaluates mechanical allodynia. Moreover, the motor coordination was also verified by the rotarod test.

3.1 Evaluation of movement evoked pain - CatWalk test

In both the saline and AAV-GFP groups there were significant differences between control and OA animals till day 14. In the OA group significant differences were also found at 7 and 14 days in comparison with t_0, as expected, confirming the development of nociception due to OA induction. After the surgical procedure, i.e. after the AAV-GFP or the saline intra-ganglionic injection, these values remained stable throughout the entire duration of the study (Fig. 8A and B).

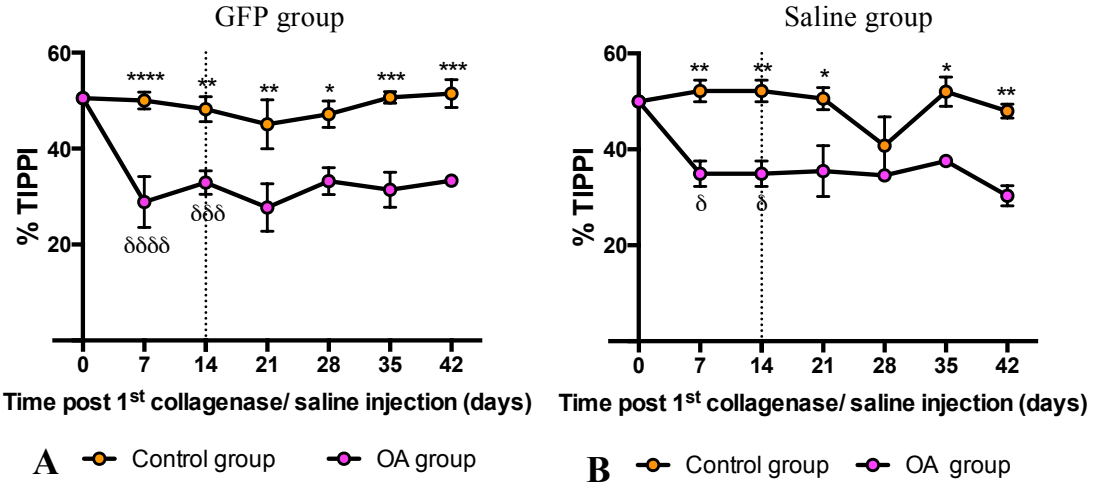

Figure 8. Evolution of the percentage of the ipsilateral paw-print total intensity of animals intra-ganglionically injected with AAV2/5-GFP or saline. Viral or saline intra-ganglionic injections were performed at 14 days (dashed lines) after collagenase or saline intra-articular injections. Graph A and B correspond to the behaviour of animals with intra-ganglionic injection of AAV-GFP and saline, respectively. Mean ± SEM, two-way ANOVA followed by Bonferroni *post-hoc* test for comparisons between the control and collagenase groups at each time-point, $^{*}p < 0.05$; $^{**}p<0.01$; $^{***}p<0.001$; $^{****}p<0.0001$. Repeated-measures followed by Bonferroni *post-hoc* test for comparisons within the same group, $^{\delta}p<0.05$; $^{\delta\delta\delta}p<0.001$; $^{\delta\delta\delta\delta}p<0.0001$ significantly different from t_0.

3.2 Evaluation of movement evoked pain - Knee-Bend

Control animals with intra-ganglionic injection of AAV-GFP (Fig. 9A) and saline (Fig. 10A) showed no differences in the Knee-Bend score throughout the study except at day 21, the first behavioural testing day after the intra-ganglionic injection, when an increase in the ipsilateral Knee-Bend score was observed (Fig. 9A and 10A). Regarding OA animals injected with AAV-GFP, an increase in the ipsilateral Knee-Bend score was observed at days 7 and 14, remaining relatively stable thereafter, with

no significant differences regarding to t_{14}, and significantly different from the contralateral knee except at day 28 (Fig 9B). In the OA group of saline intra-ganglionic injection there was also an increase in the Knee-Bend score when compared to the contralateral knee and to t_0, though not statistically significant (Fig. 10B). When comparing the Knee-Bend scores of the ipsilateral knees between OA and control animals after GFP injection significant differences were detected throughout the study, particularly at days 21, 35 and 42 after intra-articular injection (Fig. 9C).

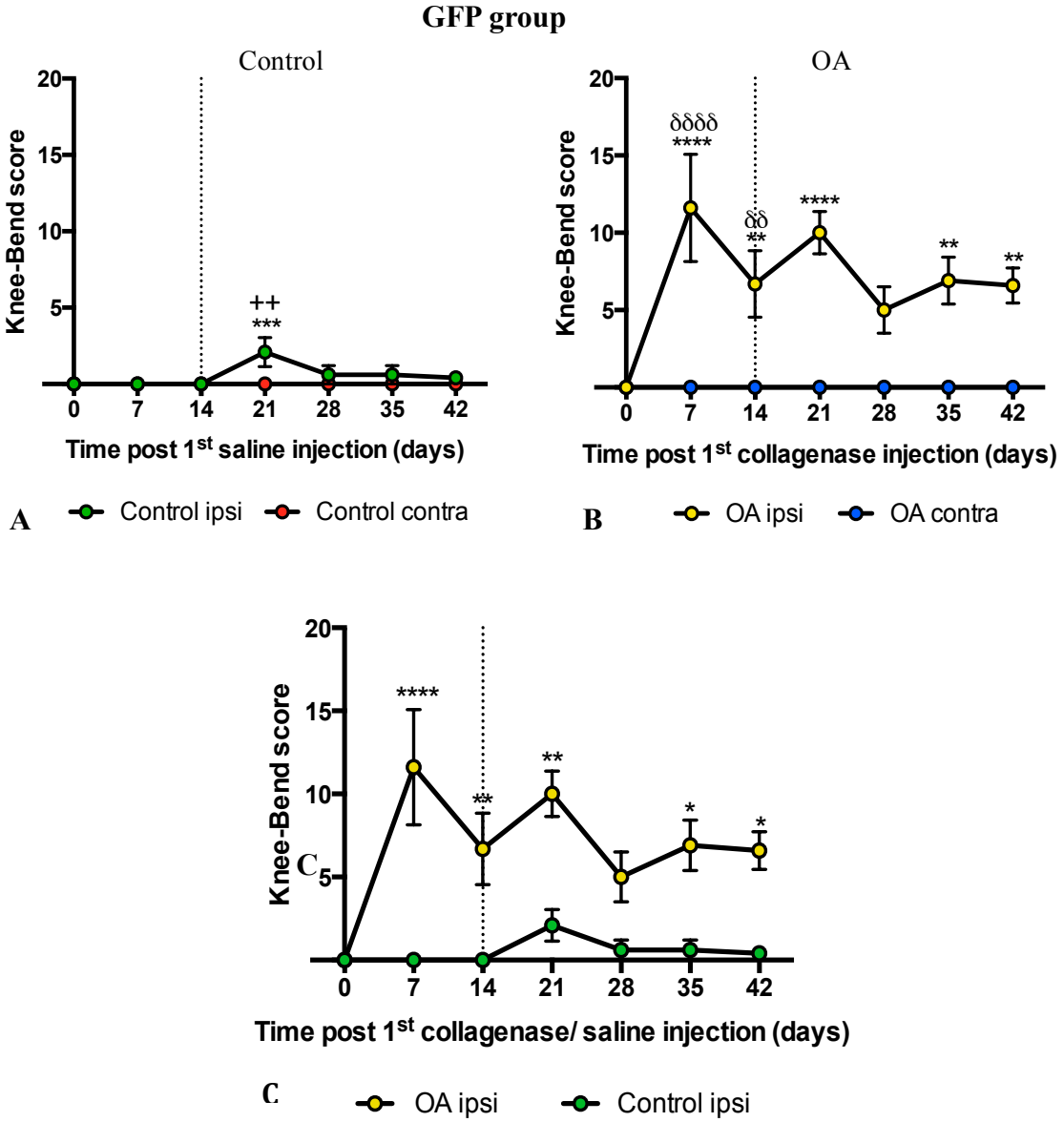

Figure 9. Knee-Bend scores of animals intra-ganglionically injected with AAV2/5-GFP. Knee-Bend scores of animals with saline intra-articular injection (control, A), animals injected with 500U of collagenase (OA, B) and Knee-Bend scores of osteoarthritic and control animals, only in the ipsilateral paw (C). Dashed line represents viral injections. Mean

± SEM, two-way ANOVA followed by the Bonferroni post hoc test for comparisons between the ipsi- and contralateral sides or between groups at each time-point, *p<0.05; **p<0.01; ***p<0.001; ****p<0.0001. Repeated-measures followed by Bonferroni *post-hoc* test for comparisons within the same group, $^{++}$P<0.01, significantly different from t_{14} and $^{\delta\delta}$p<0.01; $^{\delta\delta\delta\delta}$p<0.0001, significantly different from baseline levels (t_0).

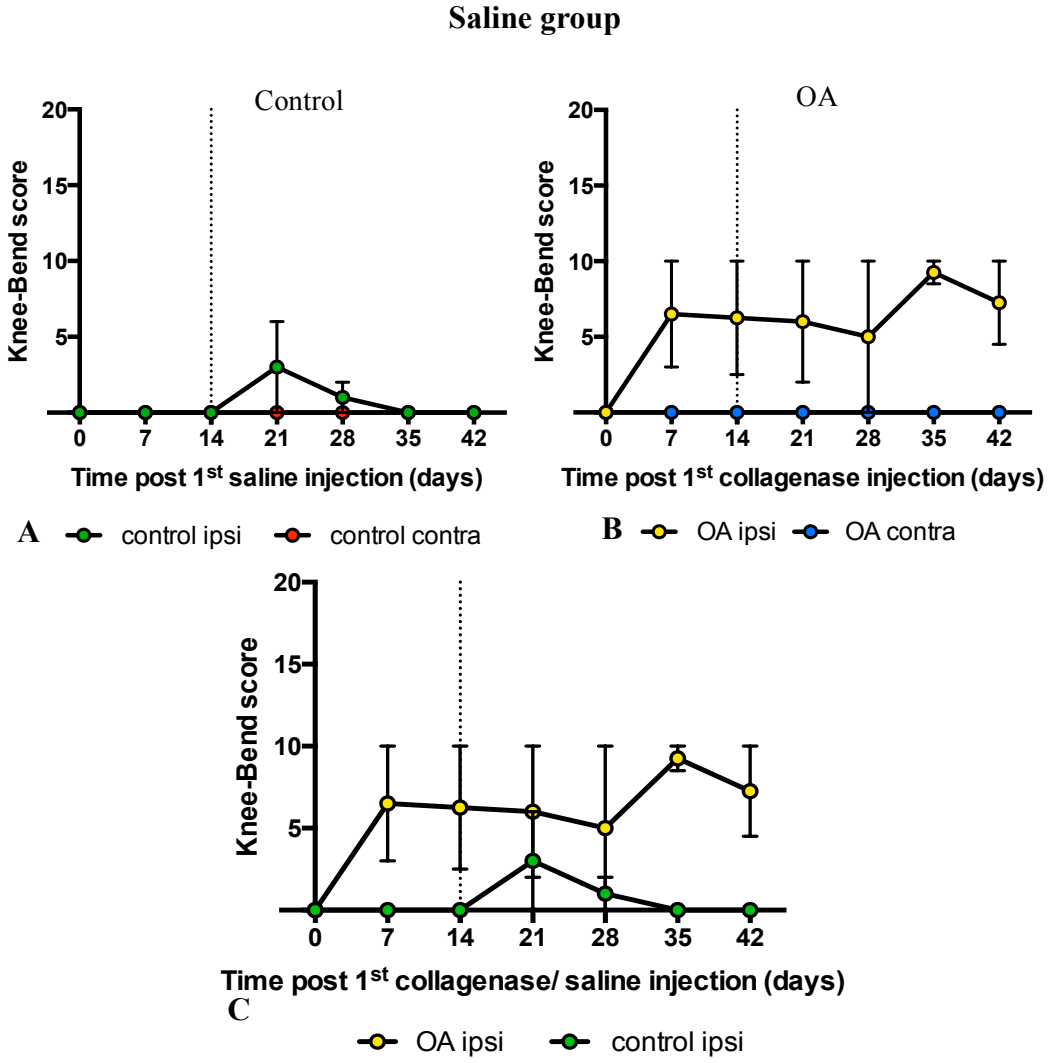

Figure 10. Knee-Bend scores of animals intra-ganglionically injected with Saline. Knee-Bend scores of animals with saline intra-articular injection (control, A), animals injected with 500U of collagenase (OA, B) and Knee-Bend scores of osteoarthritic and control animals, only in the ipsilateral paw (C). Dashed line represents saline intra-ganglionic injections. Mean ± SEM, two-way ANOVA followed by the Bonferroni post hoc test for comparisons between the ipsi- and contralateral sides or between groups at each time-point. Repeated-measures followed by Bonferroni *post-hoc* test for comparisons within the same group. No significant differences were found.

3.3 Assessment of mechanical allodynia - Von Frey test

The control animals of both groups (GFP and saline) did not show any significant differences in the PWT throughout the study as well as nor between the ipsilateral and contralateral sides (Fig. 11A and 12A). The OA animals showed a decrease in the ipsilateral PWT from day 0 onwards, that was significantly different form the contralateral side at some time-points (Fig 11B and 12B). In the GFP group these differences were statistically significant at 21 days ($p<0.01$), with a decrease in PWT of ipsilateral paw after intra-ganglionic injection, and at 42 days ($p<0.05$) (Fig. 11B). In the saline group the significant differences between the contralateral and ipsilateral sides were observed at 21 days ($p<0.01$) and at 35 days ($p<0.01$) (Fig. 12B). When comparing the ipsilateral sides between the OA and control animals of saline and GFP groups there were no statistically differences in PWT (Fig. 11C and 12C), although in the GFP group the PWT of OA animals was always inferior to that of control animals.

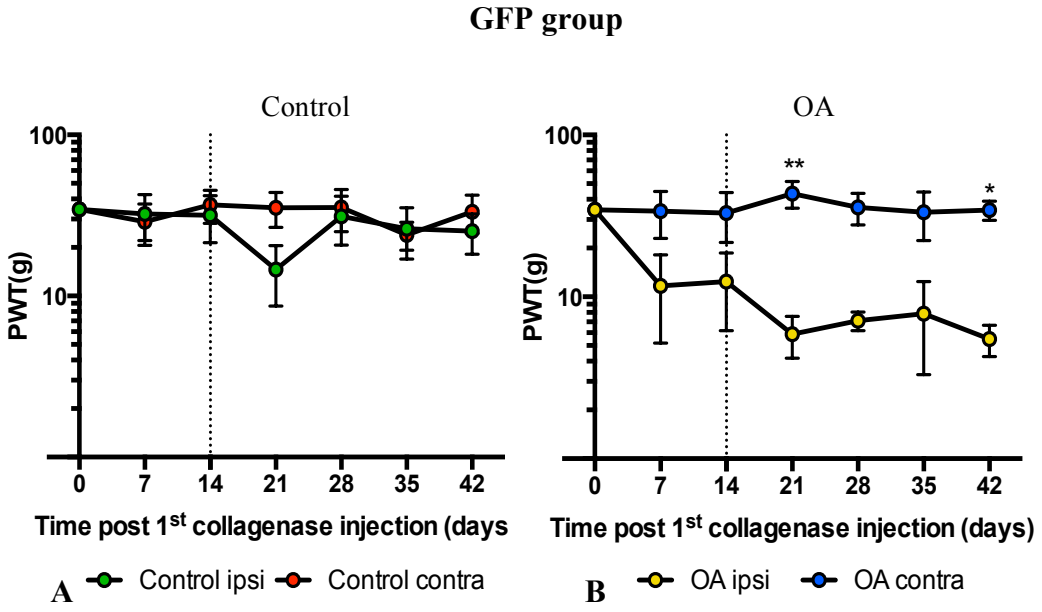

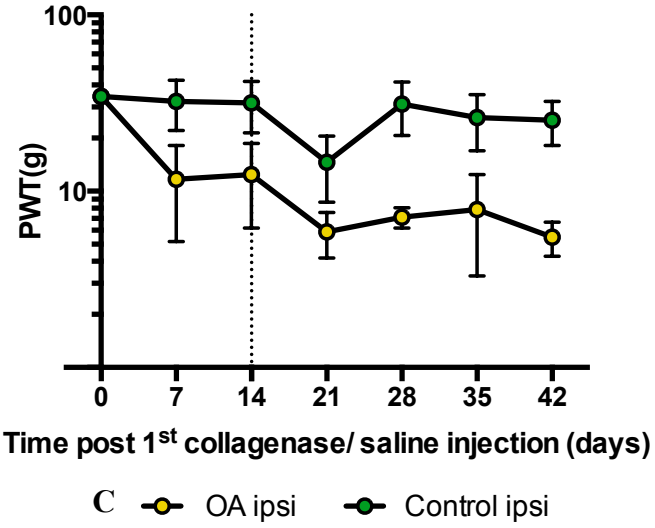

Figure 11. Paw withdrawal threshold (PWT) to Von Frey filaments of animals intra-ganglionically injected with AAV2/5-GFP. PWT of animals with saline intra-articular injection (control, A), animals injected with 500 U of collagenase (OA, B) and of osteoarthritic and control animals, only in the ipsilateral paw (C). Dashed line represents AAV2/5-GFP intra-ganglionic injections. Mean ± SEM, 2-way ANOVA followed by the Bonferroni *post-hoc* for comparisons between the ipsilateral and contralateral sides or between groups at each time point $^{*}p<0.05$; $^{**}p<0.01$. Repeated-measures followed by Bonferroni *post-hoc* test for comparisons within the same group was also performed but no statistically significant differences were found.

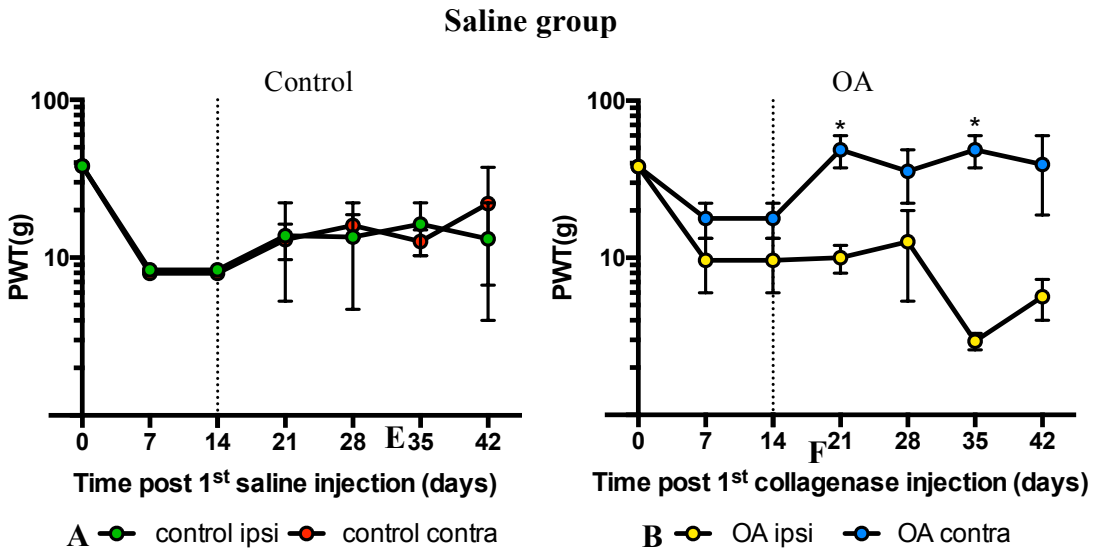

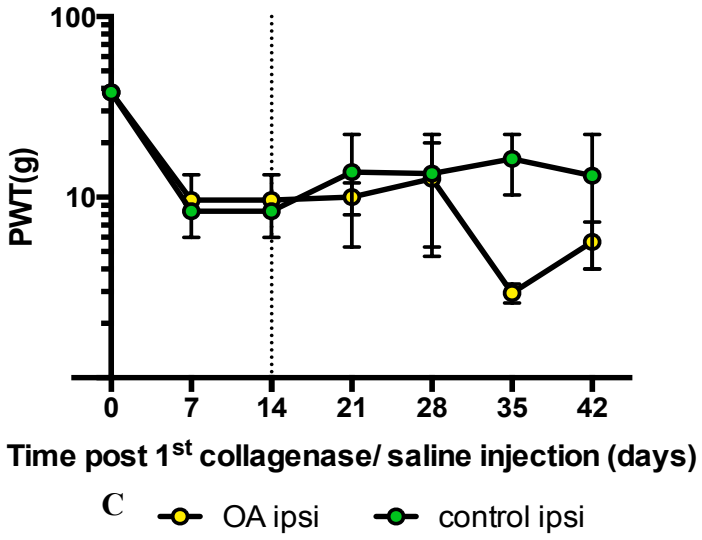

Figure 12. Paw withdrawal threshold (PWT) to Von Frey filaments of animals intra-ganglionically injected with saline. PWT of animals with saline intra-articular injection (control, A), animals injected with 500 U of collagenase (OA, B) and of osteoarthritic and control animals, only in the ipsilateral paw (C). Dashed line represents saline intra-ganglionic injections. Mean ± SEM, 2-way ANOVA followed by the Bonferroni *post-hoc* for comparisons between the ipsilateral and contralateral sides or between groups ate each time point $^{*}p<0.05$. Repeated-measures followed by Bonferroni *post-hoc* test for comparisons within the same group was also performed but no statistically significant differences were found.

3.4 Assessment of motor coordination - Rotarod test

There were no significant differences in the permanence time of animals in the rotarod, between OA and control animals of both groups (GFP and saline) throughout the study (Fig. 13 A and B).

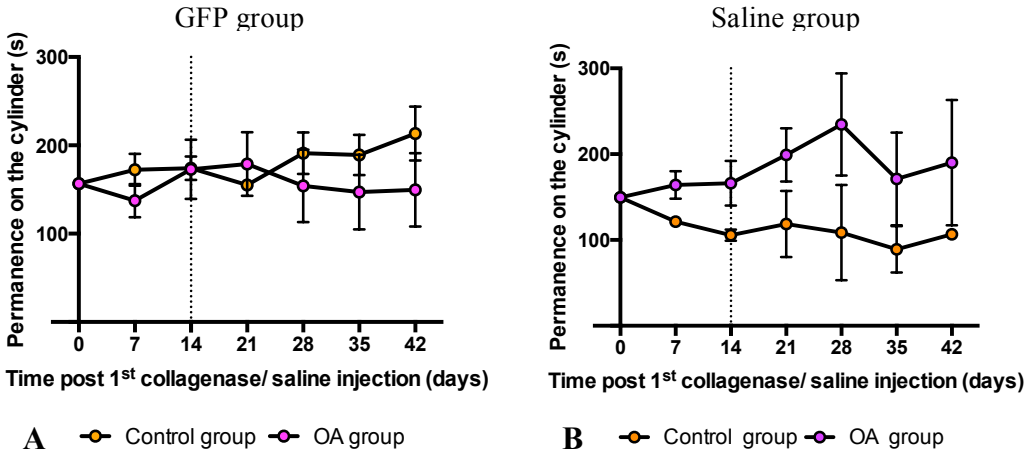

Figure 13. Permanence in Rotarod in seconds (s) of control and osteoarthritic animals following saline and AAV-GFP injections. The dashed line represents the intra-ganglionic injection of GFP (A) or saline (B). Mean ± SEM, 2-way ANOVA followed by the Bonferroni *post-hoc* test for comparisons between groups at each time-point. Repeated-measures followed by Bonferroni *post-hoc* test for comparisons within the same group. No significant differences were found.

4. Evaluation of animals´ behaviour following AAV-SPRR1A intra-ganglionic injection

At 14 days after saline or collagenase intra-articular administration an intra-ganglionic injection of AAV2/5-SPRR1A was performed in another group of control and OA animals. The animals were then subjected to the same behavioural tests performed in the AAV-GFP and saline groups.

4.1 Evaluation of movement evoked pain- CatWalk test

The CatWalk test was always performed first to minimize the effect of the manipulation of the affected knee joint in the gait of the animal. CatWalk data are presented as the percentage of the total paw print intensity (%TIPPI) (Fig. 15). Throughout the study, the control animals showed no significant changes in the paw print intensity (Fig. 14 A and C and Fig. 15). Contrariwise, in animals with OA a decrease of the %TIPPI was observed at 7 days, corresponding to an expected development of OA-associated movement and loading nociception due to collagenase injection (Fig. 15), which was significantly different from baseline (t_0) ($p<0.0001$). This can be observed in Fig. 14B showing that at 7 days after collagenase injection the area of the ipsilateral paw in contact with the floor was reduced. Differences in comparison to baseline remained significant at 14 days ($p<0.001$), before intra-ganglionic injection of AAV2/5. After AAV2/5 injection control animals did not show any differences in %TIPPI, while in OA animals an increase in %TIPPI was observed from day 28 till the end of the study, , although not reaching significance when compared to t_{14}.

As expected, significant differences were observed in %TIPPI between the control and OA animals, especially at early time-points (t7, $p<0.0001$). These differences started to decrease with the course of the study ($p<0.05$ at 14, 21 and 35 days). In fact, in the last day of the test, when SPRR1A is transduced at higher levels,

there were no significant differences between control and OA animals, with values of % of ipsilateral intensity being very similar in the two groups (Fig. 15).

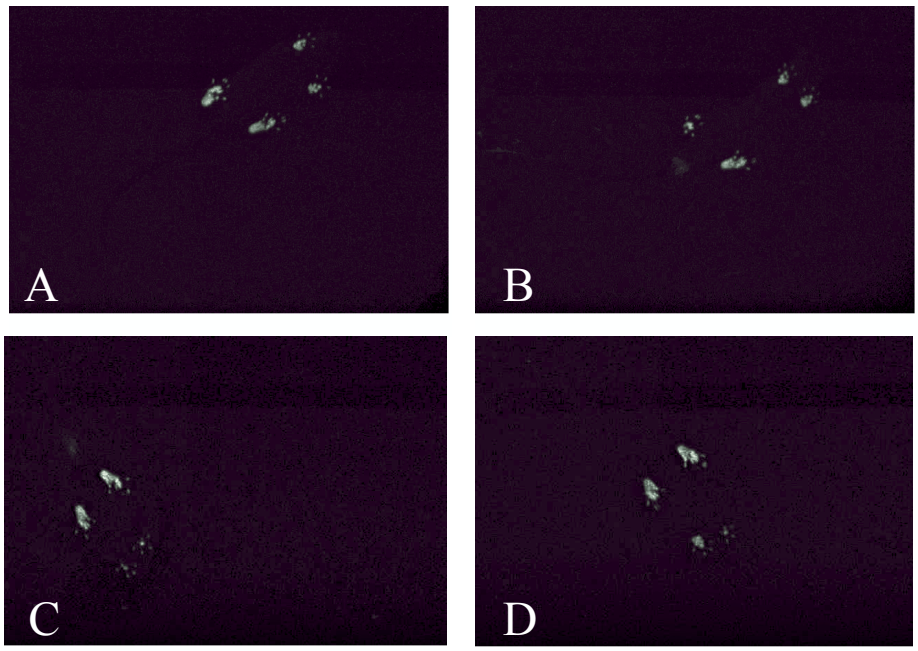

Figure 14. Image of paw prints of control (A **and** C**) and osteoarthritic animals injected with 500U of collagenase (**B **and** D**).** Images A and B correspond to 7 days after saline and collagenase injections, respectively and images C and D correspond to 4 weeks (28 days) after AAV2/5-SPRR1A intra-ganglionic injection.

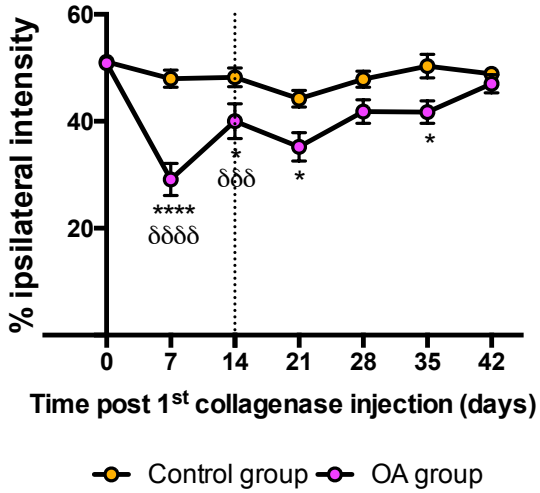

Figure 15. CatWalk data were expressed as the percentage of total ipsilateral paw print intensity (%TIPPI). Viral injections were performed at 14 days (dashed line) after collagenase or saline injection. Mean ± SEM, two-way ANOVA followed by the Bonferroni *post-hoc* test for comparisons between the control and collagenase groups at each time-point, $^{*}p<0.05$; $^{****}p< 0.001$. Repeated-measures followed by Bonferroni *post-hoc* test for

comparisons within the same group, $^{\delta\delta\delta\delta}$ $p<0.0001$,$^{\delta\delta\delta}p<0.001$, significantly different from baseline levels.

4.2 Evaluation of movement evoked pain - Knee-Bend test

The Knee-Bend test was also used to evaluate movement-induced nociception and the results are presented as a Knee-Bend score. There were no significant changes in the Knee-Bend score between the ipsilateral and contralateral knees of control animals during the study; nevertheless, the ipsilateral knee showed slightly higher values (non-significant) after intra-ganglionic injection (t_{14}) in the ipsi L4 and L5 ganglia (Fig. 16A). In contrast, in the OA group there were significant differences in the Knee-Bend score between the contralateral and ipsilateral knees, as expected. A statistically significant increase in the ipsilateral Knee-Bend score ($p<0.0001$) regarding to baseline scores (t_0) was observed, confirming a proper induction of OA and of the associated nociception, values remaining highly significant in the ipsilateral knee until 1 week after AAV2/5 injection (day 21; $p<0.0001$). Thereafter, the ipsilateral Knee-Bend score values start to decrease and at 4 weeks (t_{42}) after intra-ganglionic injection of the AAV2/5-SPRR1A the differences between both knees, although significant, were much more attenuated ($p<0.001$). In fact, after SPRR1A injection at day 14, the ipsilateral Knee-Bend score at 35 days (3 weeks after AVV2/5-SPRR1A delivery) and at 42 days, the last day of the study, were significantly different from t14 ($p<0.01$ and $p<0.001$, respectively for days 35 and 42; Fig. 16B). When comparing the ipsilateral Knee-Bend score of control and OA animals, it was observed a decrease of the differences between both groups throughout the study, so that significant differences between the ipsilateral score of the two groups were no longer detected at 42 days (Fig. 16C).

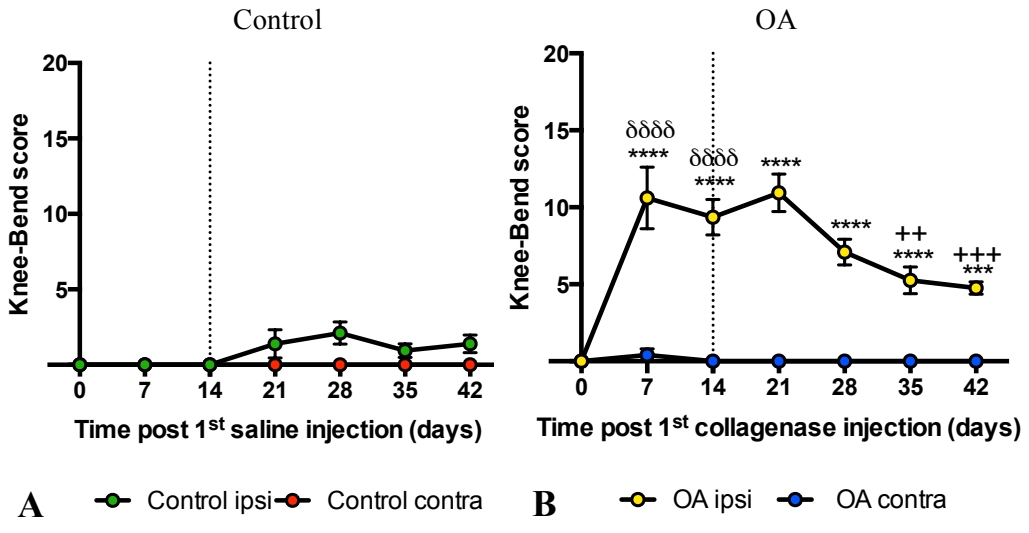

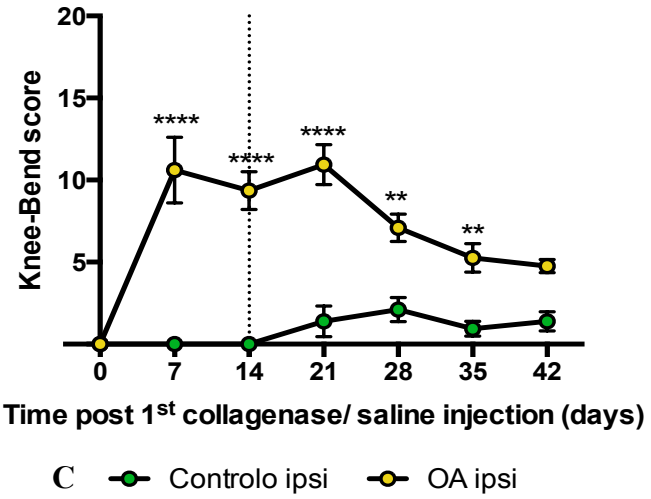

Figure 16. Knee-Bend scores of animals intra-ganglionically injected with AAV2/5-SPRR1A. Knee-Bend scores of animals injected with sterile saline (control, A), animals injected with 500 U of collagenase (OA, B) and Knee-Bend scores of osteoarthritic and control animals, only of the ipsilateral paw (C). The dashed lines represent the intra-ganglionic injections of AAV-SPRR1A. Mean ± SEM, 2-way ANOVA followed by the Bonferroni *post-hoc* test for comparisons between the ipsi and contralateral sides or between groups at each time-point, $^{**}p<0.01$; $^{***}p<0.001$; $^{****}p<0.0001$. Repeated-measures followed by the Bonferroni *post-hoc* test for comparisons within the same group, $^{\delta\delta\delta\delta}p<0.0001$, significantly different from baseline levels (t_0) and $^{++}p<0.01$, $^{+++}p<0.001$, significantly different from t_{14}.

4.3 Assessment of mechanical allodynia - Von Frey test

Von Frey test was used to evaluate the mechanical allodynia of the animals and results are presented as paw withdrawal threshold (PWT). In control animals, a decrease in the PWT in the ipsilateral paw was observed after the intra-ganglionic injection (t_{14}) being significantly different from t_{14} at t_{21} ($p<0.001$) and t_{28} ($p<0.01$), and also significantly different from the contralateral side at t_{21} (Fig. 17A). However, at the latter time-points the differences disappeared. Throughout the study, yet, no differences were observed in the contralateral PWT. In the OA group the contralateral side also showed similar PWT values throughout the study and the reductions observed on the ipsilateral side at 7 and 14 days were statistically different from baseline levels ($p<0.0001$) and from the contralateral paw ($p<0.0001$ and $p<0.01$, for the 7 and 14 days, respectively), demonstrating a successful OA induction. After AAV2/5 injection, although significant differences in the PWT between the ipsilateral

and contralateral sides were still observed, significant differences in ipsilateral PWT regarding to t_{14} were no longer detected, indicating an attenuation of mechanical allodynia (Fig. 17B). When comparing the ipsilateral side of both groups, highly significant differences were observed until t_{14} ($p<0.0001$), as expected. However, from this time onwards the differences between the ipsilateral sides become less evident until t_{42} (Fig. 17C).

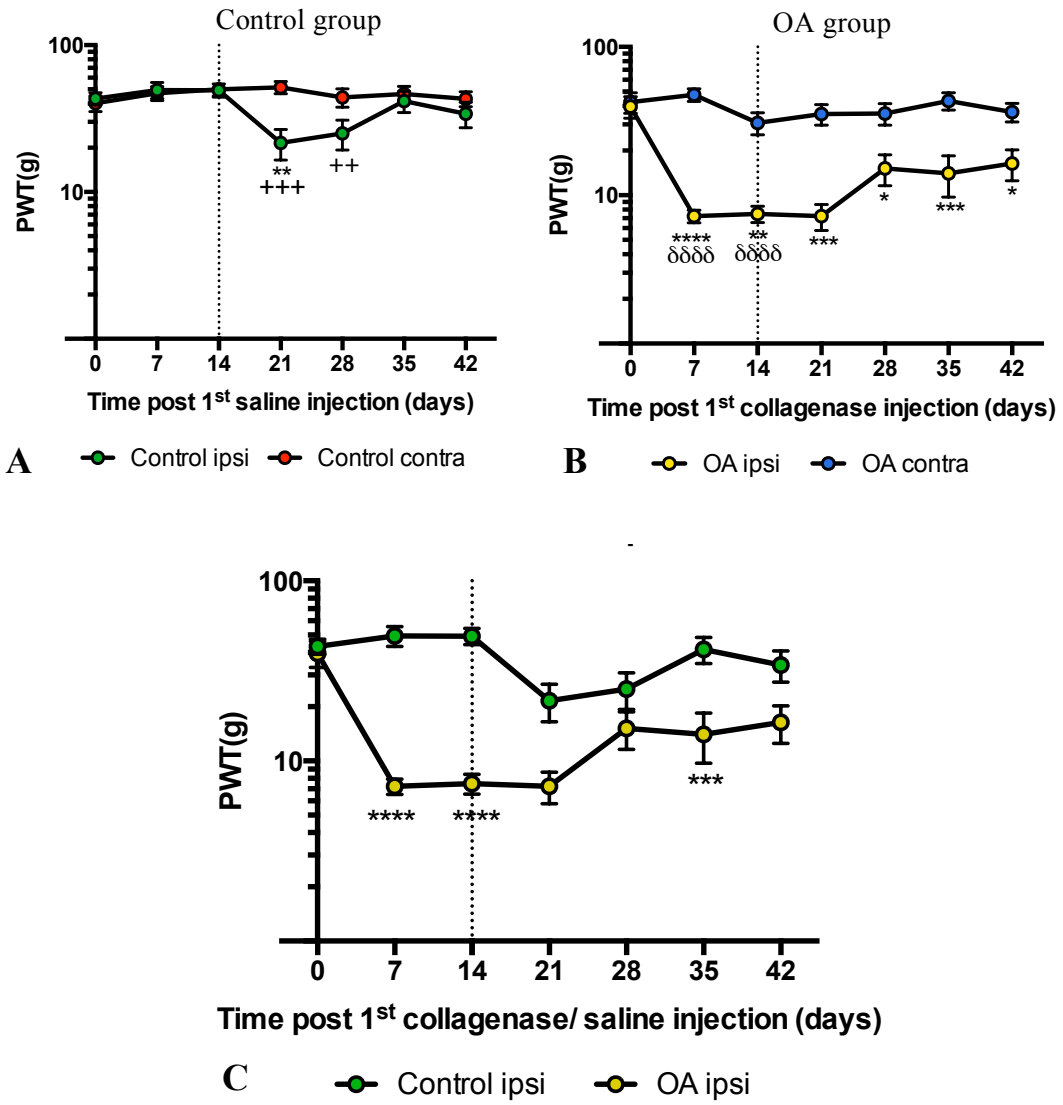

Figure 17. Paw withdrawal threshold (PWT) to Von Frey filaments of animals intra-ganglionically injected with AAV2/5-SPRR1A. PWT to Von Frey filaments in control (A) and osteoarthritic animals (B). Graph C represents the PWT of the ipsilateral paw in both groups. The dashed lines represent the intra-ganglionic injections of AAV-SPRR1A. Mean ±SEM, 2-way ANOVA followed by the Bonferroni post-hoc for comparisons between the

the ipsilateral and contralateral sides or between groups at each time point $^{*}p < 0.05$; $^{**}p < 0.01$; $^{***}p<0.001$; $^{****}p<0.0001$. Repeated-measures followed by the Bonferroni *post-hoc* test for comparisons within the same group, $^{\delta\delta\delta\delta}P<0.0001$, significantly different from baseline levels (t_0) and $^{++}p<0.01$, $^{+++}p<0.001$, significantly different from t14.

4.4 Assessment of motor coordination- Rotarod test

No differences were observed throughout the study in none of the two groups of animals as well as no differences between them. These results showed that the locomotor capacity of the animals was not compromised by the AAV-SPRR1A intra-ganglionic injections (Fig. 18)

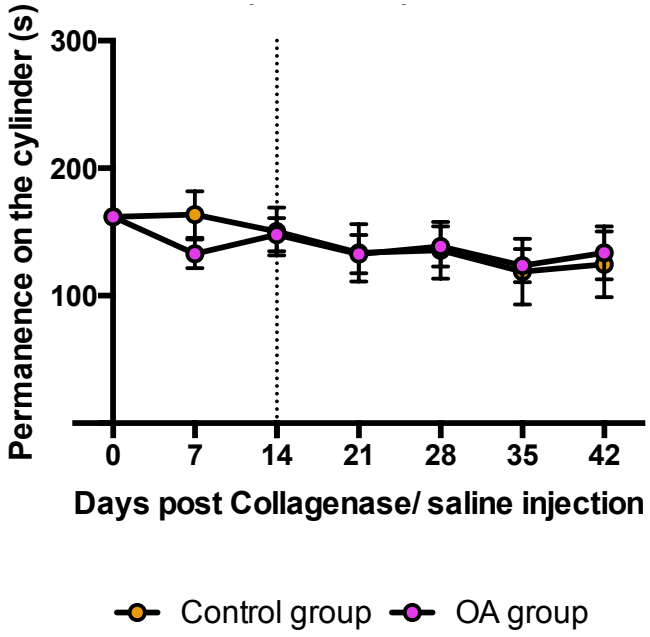

Figure 18. Permanence on Rotarod in seconds (s) of control and osteoarthritic groups following AAV2/5-SPRR1A. The dashed line represents the intra-ganglionic injection of AAV-SPRR1A. Mean ± SEM, 2-way ANOVA followed by the Bonferroni *post-hoc* test for comparisons between groups at each time-point. Repeated-measures followed by Bonferroni *post-hoc* test for comparisons within the same group. No significant differences were found.

5. Behaviour of osteoarthritic animals of all groups (SPRR1A, GFP and saline)

When comparing all the OA animals used, after intra-ganglionic injection of AAV-SPRR1A, AAV-GFP or saline, significant differences between the AAV-GFP and AAV-SPRR1A groups were observed immediately 1 week after the injections ($p<0.05$ at 21 days) in the CatWalk test, with the AAV-SPRR1A animals showing an

increase in the % of TIPPI that remained until the end of the study ($p<0.0001$ at day 42). In fact, at 42 days the SPRR1A group was also highly significantly different from the saline group ($p<0.001$; Fig. 19A). In the Knee-Bend test, as well as in the Von Frey test, there were no statistically significant differences between groups (Fig. 19B and C). In the rotarod test there were only significant differences between the SPRR1A and saline groups at 28 days of the study (Fig. 19D).

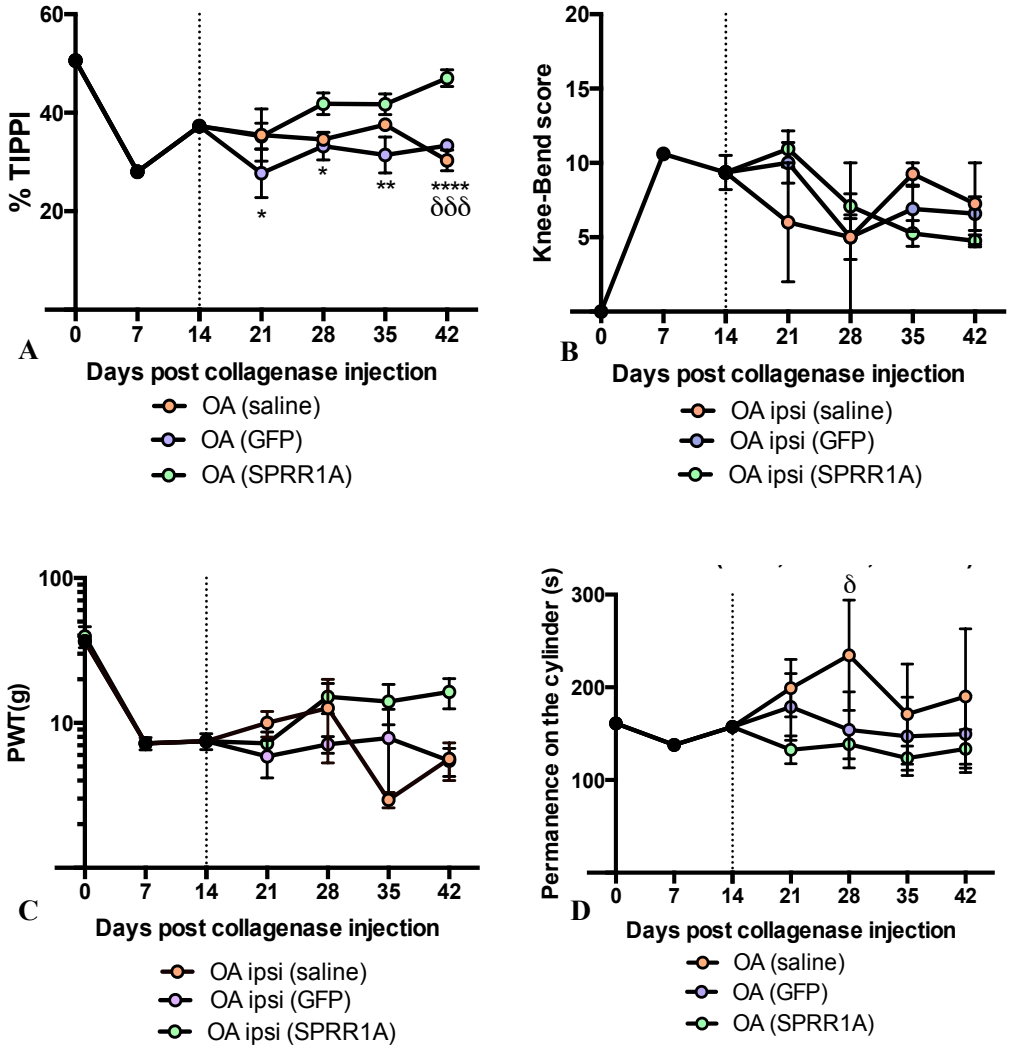

Figure 19. Behaviour of OA animals of SPRR1A, GFP and saline groups. CatWalk data of OA animals (A). Ipsilateral Knee-Bend scores of OA animals (B). Paw withdrawal thresholds (PWT) in the ipsilateral side of OA animals (C) and time of permanence in the rotarod apparatus of the OA animals (D). Mean ± SEM, 2-way ANOVA followed by the Bonferroni *post-hoc* test for comparisons between groups at each time-point, *$p<0.05$; **$p<0.01$; ****$p<0.0001$ for differences between the SPRR1A and GFP groups; $^{\delta}p<0.05$; $^{\delta\delta\delta}p<0.001$ for differences between the SPRR1A and saline groups

6. Evaluation of gene expression

6.1 Real time qPCR for SPRR1A

Gene expression analysis in L4 and L5 DRGs by real time qPCR was employed to evaluate and confirm the overexpression of SPRR1A after intra-ganglionic injection of AAV-SPRR1A. Furthermore, SPRR1A mRNA levels were also quantified in L4 and L5 DRGs of animals submitted to intra-ganglionic injections of saline and AAV-GFP. Results showed high levels of SPRR1A overexpression in L4 and L5 ipsilateral DRGs of control and OA animals following AAV-SPRR1A injection; however, the levels of overexpression were much higher in control animals ($p<0.05$; Fig. 20A). Regarding to the saline and AAV-GFP groups there was also an upregulation of the mRNA levels of SPRR1A in L4 and L5 ipsilateral DRGs of both control and OA animals (Fig. 20B and C). In the AAV-GFP group the ipsilateral DRGs of OA animals presented higher levels of SPRR1A expression comparatively to ipsilateral DRGs of control animals, although not statistically significant (Fig. 20B). On the other hand, in the saline group the opposite occurred, with the expression of SPRR1A in ipsilateral DRGs of control animals being statistically greater than in OA animals ($p<0.05$; Fig. 20C).

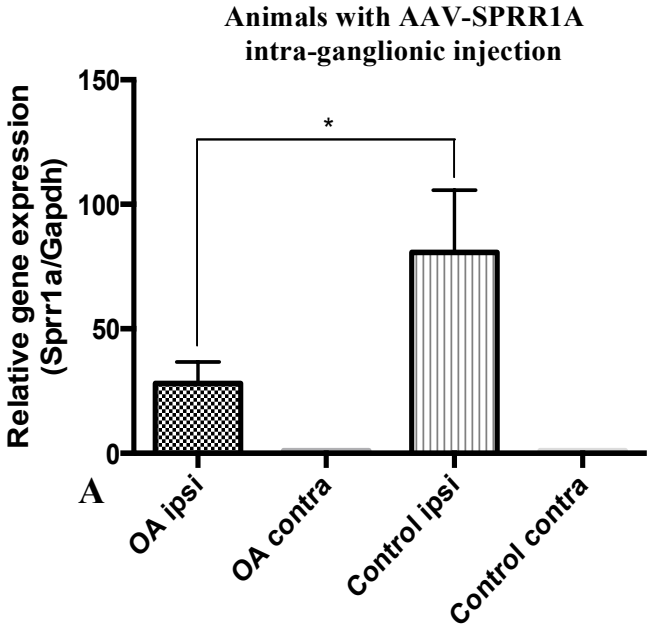

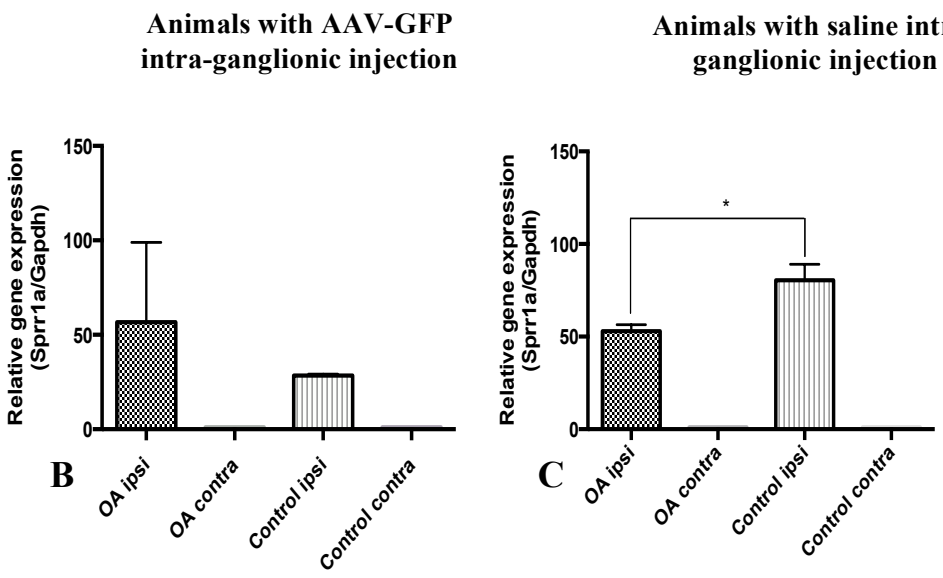

Figure 20. Gene expression studies for SPRR1A. The levels of SPRR1A mRNA expression in the L4 and L5 of control and OA animals with an intra-ganglionic injection of AAV-SPRR1A (n=10; 5 OA animals, 5 control animals) (A), AAV-GFP (n=4, 2 OA animals, 2 control animals) (B) or saline (n=4, 2 OA animals, 2 control animals) (C) were measured by real time quantitative PCR. The expression of SPRR1A was assessed 4 weeks after intra-ganglionic injections. Target gene expression was normalized to the expression of *Gapdh*. Mean ± SEM, one-way ANOVA followed by the Bonferroni *post-hoc* test, *p<0.05.

6.2 Real time qPCR for ATF-3 and GFAP

In L4 and L5 DRGs injected with AAV-SPRR1A, the mRNA expression of GFAP and ATF-3 genes was also evaluated. As previously stated, ATF-3 is described as being part of the same regeneration pathway of SPRR1A, while GFAP is a marker of SGCs activation that showed increased levels in DRGs innervating the knee joint after OA induction by collagenase intra-articular injection (Adaes *et al.*, 2017). Our real time qPCR analyses showed an increase in the mRNA expression of GFAP and ATF-3 in ipsilateral L4 and L5 DRGs of control and OA animals, 4 weeks after intra-ganglionic injection of AAV-SPRR1A. The expression of both genes was higher in ipsilateral DRGs of control animals (Fig. 21A and B), with the levels of ATF-3 presenting statistically significant increases in comparison to those in OA animals ($p<0.05$; Fig. 21B).

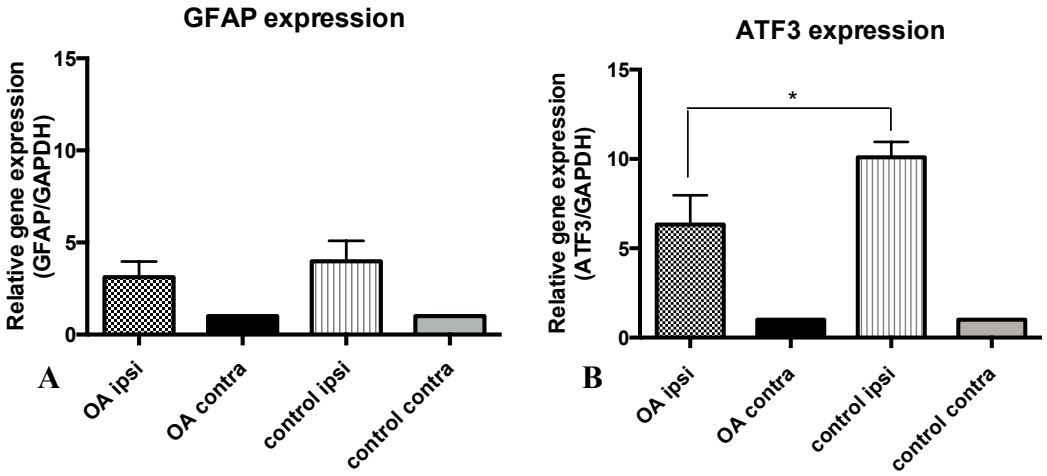

Figure 21. Gene expression studies for GFAP and ATF-3. The expression of GFAP (A) and ATF-3 (B) in the ipsilateral and contralateral L4 and L5 DRGs of control (n=5) and OA (n=5) animals was measured by real time quantitative PCR, 4 weeks after intra-ganglionic injection of AAV-SPRR1A. Target gene expression was normalized to the expression of *Gapdh*. Mean ± SEM, one-way ANOVA followed by the Bonferroni *post-hoc* test, *p<0.05.

7. Histological analysis of the knee joint

The Fast Green and Safranin O method was used to ascertain whether there were histopathological changes in the knee joints of OA animals following intra-ganglionic injections of AAV-SPRR1A, AAV-GFP or saline. All OA animals showed a decrease in the proteoglycan content of the articular cartilage (Fig. 22A, B and C). Furthermore, OA animals injected with AAV-SPRR1A showed a slight erosion of the cartilage and consequent exposure of the subchondral bone (Fig. 22C).

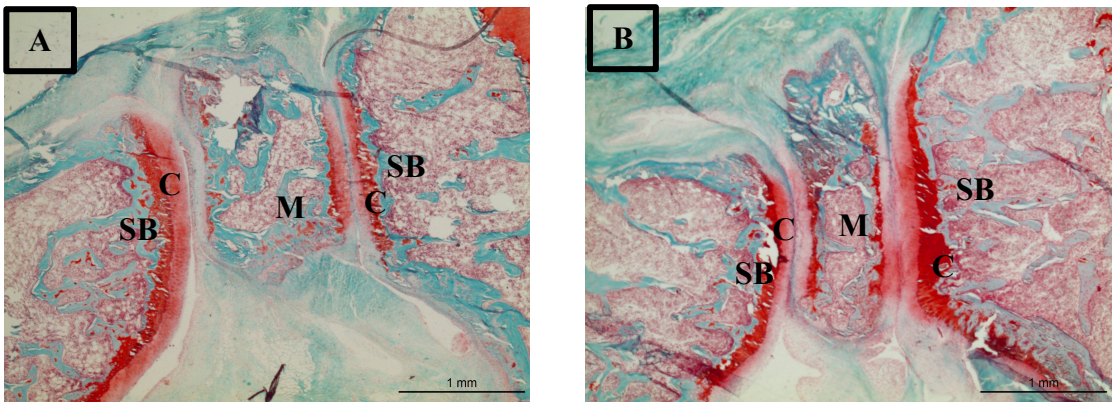

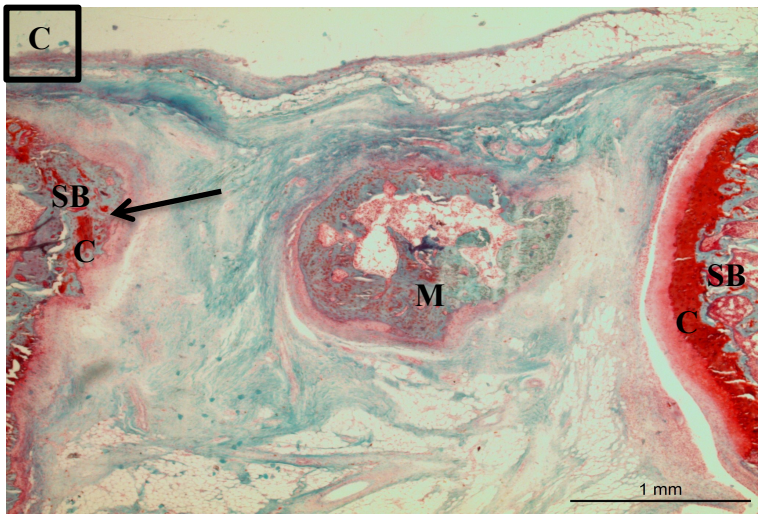

Figure 22. Histopathology of knee sections from OA animals with intra-ganglionic injection of saline (A), AAV-GFP (B) or AAV-SPRR1A (C). Sections were stained with Safranin O and Fast Green. C-articular cartilage; SB-subchondral bone; M- meniscus. The black arrow in (C) indicates a slight erosion of the cartilage and consequent exposure of the subchondral bone in OA animals receiving an intra-ganglionic injection of AAV-SPRR1A. 2,5x magnification.

Discussion

Osteoarthritis has become one of the most common health problems in the world and taking into account the inefficiency of treatments in the pain management it is extremely important to find out new treatment strategies. The expression of genes/proteins that may contribute to the regenerative capacity of the neurons has been shown to be altered in primary sensory neurons after peripheral lesions (Schreyer & Skene, 1993; Xiao *et al.*, 2002). Furthermore, there are some studies demonstrating an increase in the SPRR1A expression after peripheral injuries (Bonilla *et al.*, 2002; Starkey *et al.*, 2009) and showing the role of its increase in promoting axonal outgrowth in DRG neurons (Bonilla *et al.*, 2002). In an experimental model of knee OA induced by collagenase injection we also have found increased SPRR1A mRNA and protein levels in the ipsilateral DRG neurons (Adães *et al*., unpublished data). Altogether, these findings encouraged us to evaluate the effect of SPRR1A on the nociceptive behaviour of these OA rats. For that purpose we decided to use rAAV vectors to stimulate the overexpression of SPRR1A in primary sensory neurons.

Lately, rAAV vectors have been widely used in gene delivery on primary sensory neurons by direct injection into the DRG. Several AAV serotypes are used, yet, it was shown that the AAV2/5 has the best performance, transducing >90% of DRG neurons (Mason *et al.*, 2010). In our investigation, we used this serotype to transfer our gene of interest (*Sprr1a*) into the DRG. Preliminary studies using other injection targets rather than the DRGs, such as knee joint, subcutaneous, intraspinal or intrathecal injections indicated that the best approach to achieve a satisfactory level of transfection efficiency would be to do intra-ganglionic injections, albeit being a highly invasive procedure. In order to find out the best time for an efficient transfection of AAV2/5, we started by doing intra-ganglionic injections of AAV2/5 expressing the reporter gene GFP, and assessing different times of transduction (4, 6 and 8 weeks after injection). Indeed, our results showed that at 4 weeks after injection a higher percentage of cells expressed GFP, with no significant differences regarding to the 6 and 8 weeks time points. These data showed a great efficiency of AAV2/5 in transfecting DRG neurons since it revealed a prolonged and stable transduction along time. A similar study using the AAV6 or AAV8 serotypes, and which assessed GFP expression 3 weeks and 3 months after intra-ganglionic injections, supported our data as no significant differences in the transduction rates were found in either serotypes

over time (Yu *et al.*, 2013). However, other studies contradicted our result, since they showed a direct relationship between the transduction time of AAV2/5 (Mason *et al.*, 2010) and AAV8 (Fischer *et al.*, 2011) and GFP expression. Although we have observed a high efficiency of AAV2/5 to transduce neurons, we did not analyse which type of neuronal populations in the DRG expressed GFP. Other studies by Mason and colleagues, however, demonstrated by double-immunolabelling of GFP with CGRP or with IB4, that both small peptidergic and small non-peptidergic neurons were transduced by AAV2/5 (Mason *et al.*, 2010). For the purpose of investigating if AAV2/5 would also transduce satellite glial cells, beyond neurons, we did a double immunohistochemistry reaction against GFP and GFAP and co-localization was never observed. This result was corroborated by a study using the same serotype (Mason *et al.*, 2010) and still by other using AAV6 and AAV8 (Yu *et al.*, 2013). In controversy, Fischer et al injected AAV8-GFP intra-ganglionically and found evidence of SGCs transduction (Fischer *et al.*, 2011).

To assess the consequences of AAV delivery to the cells as well as of the surgical injection procedure, intra-ganglionic injections of AAV-GFP and saline were performed in control animals. In fact, after intra-ganglionic injections of AAV-GFP the animals showed some evidences of increased nociception induced by movement (both in the CatWalk and Knee-Bend tests) and mechanical allodynia (Von-Frey test). However, these changes were slight and gradually resolved from the first week after injection. Some studies demonstrated a similar result, with animals showing a transient significant increase in mechanical allodynia after intra-ganglionic injections of AAV-GFP (Fischer *et al.*, 2011; Samad *et al.*, 2013). The animals with saline injections displayed also minor behaviours indicative of nociception induced by movement (in the Knee-Bend test) and no mechanical allodynia, and likewise, this hypersensitivity was progressively resolved from the first week after injection. However, Fisher and colleagues demonstrated that rats with PBS intra-ganglionic injection developed a temporary mechanical allodynia (Fischer *et al.*, 2011). In addition to nociceptive behaviour, we also assessed the motor coordination by the rotarod test, which revealed that the locomotor capacity of animals was not compromised by both AAV-GFP and saline injections. Fisher *et al.,* refuted, partially, our result, since they showed that animals revealed a progressive motor impairment after AAV injection, but after PBS injection the motor function was assured (Fischer *et al.*, 2011).

OA animals received as well AAV-GFP and saline injections in order to prove that the increased nociception developed with the disease would remain unaltered by these procedures. Actually, movement and loading-induced nociception and mechanical allodynia in OA persisted until the 42 days of the study, with no significant differences regarding to the day of injections (day 14 of OA). This result was corroborated by a comparable study using animals with spared nerve injury followed by AAV2/5-GFP DRG injection, where mechanical allodynia was shown to last over the entire studied time (Samad *et al.*, 2013). Another study with intrathecal injection confirmed our result since injections of AAV-GFP and saline did not reversed the hypersensitivity shown after sciatic nerve constriction (Eaton *et al.*, 2002). Furthermore, the rotarod results showed that OA induction by collagenase intra-articular injection did not compromise the motor coordination of the animals, demonstrating that this is a suitable model for studying nociception associated to OA. Finally, although the surgical procedure caused transient changes on the nociceptive behaviour of control animals, this sensitization was minimal when compared to that caused by OA, and thus, intra-ganglionic injections seem to be an appropriate approach to study the efficacy of new treatments in chronic pain targeting the sensory ganglia.

Currently, several studies have focused on strategies to combat chronic pain through gene therapy. In line with this trend, the present study had as principal goal to check the contribution of SPRR1A overexpression on the nociceptive behaviour associated to osteoarthritis. Interestingly, following intra-ganglionic injections of AAV-SPRR1A, OA animals revealed a decrease on their nociceptive behaviour, hinting an antinociceptive effect of SPRR1A. Previous results indicating that after peripheral injury the increase on the SPRR1A expression promotes axonal outgrowth (Bonilla *et al.*, 2002) together with this behavioral finding suggest that regenerative processes triggered with OA play, indeed, a role in attenuating the nociception associated with the pathology. To our best knowledge, there are no other studies associating SPRR1A to an antinociceptive effect, and therefore this constitutes a novelty that needs to be further addressed. However, other studies using AAV carrying other genes may be comparable to our. In fact, Samad et al showed that the use of DRG-targeted AAV-mediated knockdown of $Na_v1.3$ channel by *small hairpin* RNA (shRNA) resulted in the remission of neuropathic pain in rats after spared nerve injury (Samad *et al.*, 2013). Similarly, DRG injections of AAV8 carrying the

recombinant gene for the serine protease inhibitor 3, which is upregulated in DRG after nerve injury, showed as well a reduction of neuropathic pain-like behaviours in mice after spared nerve injury (Vicuna *et al.*, 2015). In addition to the direct DRG injections, AAV injections through other routes have also proved an effect in reducing neuropathic pain. For example, the intraspinal delivery of rAAV2 carrying the gene for BDNF resulted in the reversal of neuropathic pain behaviour induced by chronic constriction injury (Eaton *et al.*, 2002), and the intrathecal delivery of AAV8 serotype carrying IL-10 resulted in the reduction of neuropathic pain associated behaviour in a model of L5 spinal nerve ligation (Storek *et al.*, 2008). Our results showed that the nociceptive behaviour in OA animals was only attenuated, and not totally reversed, which can be due to the hyperexcitability of L4 and L5 DRG neurons that were not infected by the AAV 2/5 (Samad *et al.*, 2013). Even so, our data provide behavioural evidence for a contribution of SPRR1A in fighting pain in OA rats.

Concerning the gene expression studies we showed a big increase in SPRR1A mRNA levels in ipsilateral L4/L5 DRG of control and OA animals injected with AAV-SPRR1A. This result confirmed the ability of AAV2/5 to express SPRR1A in sensory neurons. Despite this, we found a rather surprising result, with an unequal SPRR1A expression between OA and control animals, with ipsilateral DRG of control animals revealing a much greater overexpression than ipsilateral DRG of OA animals. Exposure of cells to sub-optimal growth conditions can be considered as a stress and immediate responses are necessary to ensure the survival of cells in response to extracellular changes (de Nadal *et al.*, 2011). So, a possible justification is the existence of a downregulation process occurring in OA animals as a compensatory mechanism. Indeed, SPRR1A was shown to be increased in ipsilateral DRG of OA animals (Adães *et al*., unpublished data) and its overexpression by AAV-SPPR1A injection may to cause a continuous axonal growth (exogenously induced) that is no longer necessary and which eventually may have consequences, which may lead to a SPRR1A downregulation as a counteraction. In addition, we were faced with another startling result, as the animals with AAV-GFP and saline injections revealed an increase in the mRNA levels of SPRR1A of the same magnitude order as that of the animals injected with AAV-SPRR1A. Although animals with saline injection show a greater upregulation of SPRR1A in ipsilateral DRG of control animals, as in animals with AAV-SPRR1A injection, AAV-GFP animals showed a greater upregulation of SPRR1A in ipsilateral DRG of OA animals. Thus, considering these data and

knowing the role of SPRR1A in regeneration after peripheral injury, the only reasonable explanation for this data is the invasiveness of the surgical procedure for intra-ganglionic injection, that *per se* may initiate a regenerative process in response to a possible DRG lesion, which in this case is manifested by an increase in the SPRR1A expression.

ATF-3 is considered a marker of neuronal injury (Tsujino *et al.*, 2000) and more recently its expression has been associated to regenerative processes, since it was shown to promote neurite outgrowth in cultured adult DRG neurons (Seijffers *et al.*, 2006). ATF-3 transgenic mice showed increased levels of SPRR1A in DRG (Seijffers *et al.*, 2007) and likewise OA induction revealed an increase in the expression of SPRR1A within the ATF-3 population (Adães *et al*., unpublished data). These reports suggest a relationship between both genes and the possibility of they belonging to the same regeneration-inducing signalling pathway. Similarly, our result goes in line with previous data showing as well a direct relationship between SPRR1A and ATF-3, since the SPRR1A overexpression seems to increase ATF-3 levels. As in the data of SPRR1A overexpression, the ipsilateral DRG of control animals revealed a higher increase in the ATF-3 mRNA levels than ipsilateral DRG of OA animals. Thus, in addition to ATF-3 expression triggering an upregulation of SPRR1A (Seijffers *et al.*, 2007), it seems that the opposite also happens, similarly to the relationship between SPRR1A and SOX11 (Jing *et al.*, 2012).

After peripheral nerve injury, SGCs undergo activation, contributing to the maintenance of neuropathic pain (Takeda *et al.*, 2009; Liu *et al.*, 2012). It is known that after osteoarthritis induction by collagenase intra-articular injection there is glial activation in the DRG (Adaes *et al.*, 2017) and furthermore, it is known that SGCs are also activated after direct DRG injections of saline (Puljak *et al.*, 2009). Indeed, it is suggested that the activation of SGCs after intra-ganglionic injection is due to an inflammatory response triggered by the procedure. GFAP is a molecule that is up-regulated in satellite glial cells when they are activated (Takeda *et al.*, 2009) and, therefore, our results regarding the GFAP gene expression showed its increase in both ipsilateral DRG of OA and control animals following AAV-SPRR1A injection. Actually, the increase in GFAP expression was much lower than the increase in ATF-3 expression, although it remained consistent with SPRR1A and ATF-3 expression, with a slightly higher increase in control animals. These data do not seem to be corroborated by above mentioned studies, since OA animals with intra-ganglionic

injections revealed less glial activation than control animals only with DRG injection. One possible explanation for this result, as in the case of ATF-3, is the existence of a relationship between SPRR1A and GFAP. Of course to test this hypothesis further studies will be necessary, since, so far both SPRR1A and GFAP appear to have opposing roles; while SPRR1A show an antinociceptive role, glial activation is associated with pain maintenance.

Through histological analysis of the knee joint it was possible to realize if the improvement in nociceptive behaviour of OA animals by AAV-SPRR1A injection correlated with a beneficial effect in the joint. However, the results were surprising, since, although all OA animals (OA with saline injection, OA with AAV-GFP injection and OA with AAV-SPRR1A injection) showed a decrease in the proteoglycan content of articular cartilage, the OA animals receiving AAV-SPRR1A showed also a slight erosion of the cartilage and exposure of the subchondral bone. Thus, these histological findings do not seem to explain the behavioural results. Several drugs have been shown to reverse the nociceptive behaviour of OA animals (Adaes *et al.*, 2014), as well as to prevent articular degeneration (Kim *et al.*, 2012). Furthermore, some studies suggest that the correlation between pain and structural changes may me not linear (Sofat & Kuttapitiya, 2014). Indeed, NSAIDs appear to have a positive effect on joint pain, like our data with the AAV-SPRR1A suggest, but can lead to destruction of the cartilage. Similar events might be occurring following SPRR1A overexpression, which possibly explain our finding of cartilage degeneration and subchondral bone exposure (Sofat & Kuttapitiya, 2014).

Conclusions

Primary sensory neurons have revealed to be an ideal target for therapeutic gene transfer and we believe that our work contributed to clarify the limitations of this type of approach, as well the role of SPRR1A overexpression on the nociceptive behaviour of OA animals.

Molecular evidences

AAV2/5 is extremely efficient in transducing neurons, but not SGCs.

The AAV2/5 serotype showed a prolonged and stable transduction, since there were no significant differences between the three time-points studied. Although there is some controversy, our result is in accordance with many studies that use other serotypes. Furthermore, based on our data we can conclude that this type of virus only transduces neurons (although we have not shown which subpopulations), and not SGCs.

Intra-ganglionic injection promotes *per se* a regenerative process and the continuous growth triggered by SPRR1A overexpression induces a downregulation of SPRR1A in OA animals.

Our real time qPCR data showed an increase of SPRR1A mRNA levels of the same magnitude order in L4 and L5 DRG injected with AAV2/5-SPRR1A and in L4 and L5 DRG injected with AAV2/5-GFP and saline. This unexpected result made us believe that the intra-ganglionic injection, because it is an invasive procedure, could initiate a regeneration process in response to a possible DRG lesion.

Moreover, we found an uneven SPRR1A expression between OA and control animals. L4 and L5 DRG injected with AAV2/5-SPRR1A of control animals showed much greater SPRR1A expression than ipsilateral DRG of OA animals. Taking into account these data we believe a downregulation process of SPRR1A in OA animals might be occurring as a compensatory event to ensure the survival of neurons, since too much SPRR1A could promote a continuous axonal outgrowth, which may have detrimental consequences.

SPRR1A showed a direct relationship with ATF-3 and GFAP.

ATF-3 and GFAP expression was observed in DRG after OA induction and in accordance with our data, both showed their highest mRNA levels in ipsilateral DRG of control animals, as SPRR1A. So, the possibility of SPRR1A and ATF-3 belonging to the same regeneration inducing signalling pathway is suggested by our result, since the SPRR1A overexpression seems to increase the ATF-3 levels. GFAP expression, although smaller than ATF-3 expression, remained consistent with SPRR1A and ATF-3 expression. Thereby, although SPRR1A is related to regeneration process and glial activation is associated with the maintenance of pain, there seems to be a relationship between SPRR1A and GFAP expression.

Behavioural and Histological evidences

DRG injection is a secure procedure.

Regarding to the procedure we can now conclude that, although it causes some behavioural changes, they are fleeting and slight and, therefore DRG injection is a secure procedure and a valuable tool in pain research.

SPRR1A attenuates the nociceptive behaviour of OA animals.

SPRR1A did not reverse the degradation of cartilage caused by OA.

SPRR1A seems to have an antinociceptive potential in OA animals, since it caused an attenuation of their nociceptive behaviour. However, despite these behavioural evidences, the histopathological findings did not reflect this, as the knee joints of OA animals receiving an AAV-SPRR1A injection showed slight erosion of the cartilage and exposure of the subchondral bone.

Future Perspectives

We are aware that additional experiments are necessary to clarify some of our hypotheses. Based in our data we need to evaluate which subtypes of neurons are transduced by the AVV2/5 to be able to confirm our results at the behavioural level. Likewise, we need to investigate the type of relationship between the activation of SGCs and the expression of SPRR1A.

Although intra-ganglionic injection of AAV2/5-SPRR1A in OA animals has shown attenuation on their nociceptive behaviour, the intra-ganglionic procedure showed some limitations, in so far as, control animals demonstrated slight nociceptive behaviour. Furthermore, the sharp rise in the SPRR1A mRNA levels after DRG injection of AAV-GFP and saline reveal the triggering of a regenerative process due to, probably, a DRG lesion inherent to the surgical procedure. For this reason, the implementation of a new approach would be important. Lopes *et al*., proposed an alternative approach to target peripheral neurons in vivo through the injection in the gastrocnemius muscles of nanoparticles to vectorize therapeutic genes. In this study, the injection of nanoparticles mediating the delivery of BDNF, followed by peripheral nerve crush injury, showed a recovery on the thermal nociceptive function and a delay in the allodynia development (Lopes *et al.*, 2017). Furthermore, this method revealed that the BDNF mRNA levels were significantly increased in lumbar DRGs. Hence, this approach would be a good alternative to direct DRG injections.

References

Abramson, S.B. & Attur, M. (2009) Developments in the scientific understanding of osteoarthritis. *Arthritis Res Ther*, **11**, 227.

Adaes, S., Almeida, L., Potes, C.S., Ferreira, A.R., Castro-Lopes, J.M., Ferreira-Gomes, J. & Neto, F.L. (2017) Glial activation in the collagenase model of nociception associated with osteoarthritis. *Mol Pain*, **13**, 1744806916688219.

Adães, S., Almeida, L., Soares, M. L., Ferreira, A.C. & Castro-Lopes, J.M. Injury-induced expression of regeneration-associated molecules in the collagenase model of Osteoarthrits. In preparation for submission.

Adaes, S., Ferreira-Gomes, J., Mendonca, M., Almeida, L., Castro-Lopes, J.M. & Neto, F.L. (2015) Injury of primary afferent neurons may contribute to osteoarthritis induced pain: an experimental study using the collagenase model in rats. *Osteoarthritis Cartilage*, **23**, 914-924.

Adaes, S., Mendonca, M., Santos, T.N., Castro-Lopes, J.M., Ferreira-Gomes, J. & Neto, F.L. (2014) Intra-articular injection of collagenase in the knee of rats as an alternative model to study nociception associated with osteoarthritis. *Arthritis Res Ther*, **16**, R10.

Al-Safar, F.J., Gnabadi, S., Yaakub, H. & Fakurazi, S. (2009) Collagense and Sodium iodoacetate-induced experimental osteoarthritis model in Sprague Dawley Rats. *Asian Journal of Scientific Research*, **2,** 167-179.

Ahmed, A.S., Li, J., Erlandsson-Harris, H., Stark, A., Bakalkin, G. & Ahmed, M. (2012) Suppression of pain and joint destruction by inhibition of the proteasome system in experimental osteoarthritis. *Pain*, **153**, 18-26.

Ashraf, S. & Walsh, D.A. (2008) Angiogenesis in osteoarthritis. *Curr Opin Rheumatol*, **20**, 573-580.

Basbaum, A.I., Bautista, D.M., Scherrer, G. & Julius, D. (2009) Cellular and molecular mechanisms of pain. *Cell*, **139**, 267-284.

Belmonte, C. & Cervero, F. (1996) Neurobiology of nociceptors. Oxford University Press.

Berta, T., Qadri, Y., Tan, P.H. & Ji, R.R. (2017) Targeting dorsal root ganglia and primary sensory neurons for the treatment of chronic pain. *Expert Opin Ther Targets*, **21**, 695-703.

Bingham, B., Ajit, S.K., Blake, D.R. & Samad, T.A. (2009) The molecular basis of pain and its clinical implications in rheumatology. *Nat Clin Pract Rheumatol*, **5**, 28-37.

Blagojevic, M., Jinks, C., Jeffery, A. & Jordan, K.P. (2010) Risk factors for onset of osteoarthritis of the knee in older adults: a systematic review and meta-analysis. *Osteoarthritis Cartilage*, **18**, 24-33.

Blom, A.B., van Lent, P.L., Holthuysen, A.E., van der Kraan, P.M., Roth, J., van Rooijen, N. & van den Berg, W.B. (2004) Synovial lining macrophages mediate osteophyte formation during experimental osteoarthritis. *Osteoarthritis Cartilage*, **12**, 627-635.

Blom, A.B., van Lent, P.L., Libregts, S., Holthuysen, A.E., van der Kraan, P.M., van Rooijen, N. & van den Berg, W.B. (2007) Crucial role of macrophages in matrix metalloproteinase-mediated cartilage destruction during experimental osteoarthritis: involvement of matrix metalloproteinase 3. *Arthritis Rheum*, **56**, 147-157.

Bonilla, I.E., Tanabe, K. & Strittmatter, S.M. (2002) Small proline-rich repeat protein 1A is expressed by axotomized neurons and promotes axonal outgrowth. *J Neurosci*, **22**, 1303-1315.

Bonin, R.P., Bories, C. & De Koninck, Y. (2014) A simplified up-down method (SUDO) for measuring mechanical nociception in rodents using von Frey filaments. *Mol Pain*, **10**, 26.

Boulis, N.M., Noordmans, A.J., Song, D.K., Imperiale, M.J., Rubin, A., Leone, P., During, M. & Feldman, E.L. (2003) Adeno-associated viral vector gene expression in the adult rat spinal cord following remote vector delivery. *Neurobiol Dis*, **14**, 535-541.

Brandt, K.D. (2002) Animalbe models of osteoarthritis. *Biorheology*, **39**, 221-235.

Buller, R.M., Janik, J.E., Sebring, E.D. & Rose, J.A. (1981) Herpes simplex virus types 1 and 2 completely help adenovirus-associated virus replication. *J Virol*, **40**, 241-247.

Carpenter, B., Hill, K.J., Charalambous, M., Wagner, K.J., Lahiri, D., James, D.I., Andersen, J.S., Schumacher, V., Royer-Pokora, B., Mann, M., Ward, A. & Roberts, S.G. (2004) BASP1 is a transcriptional cosuppressor for the Wilms' tumor suppressor protein WT1. *Mol Cell Biol*, **24**, 537-549.

Castro-Lopes J.M. & Neto F. (2014) Neurobiology of nociceptors. In: Pain 2014: Refresher Courses, 15th World Congress on Pain, Chapter 39, pp. 407-419 (Raja S.N. and Sommer C.L., Ed.), IASP Press, Washington, D.C.

Chevalier, X., Eymard, F. & Richette, P. (2013) Biologic agents in osteoarthritis: hopes and disappointments. *Nat Rev Rheumatol*, **9**, 400-410.

Console-Bram, L.M., Fitzpatrick-McElligott, S.G. & McElligott, J.G. (1996) Distribution of GAP-43 mRNA in the immature and adult cerebellum: a role for GAP-43 in cerebellar development and neuroplasticity. *Brain Res Dev Brain Res*, **95**, 97-106.

Cooper, T.E., Chen, J., Wiffen, P.J., Derry, S., Carr, D.B., Aldington, D., Cole, P. & Moore, R.A. (2017) Morphine for chronic neuropathic pain in adults. *Cochrane Database Syst Rev*, **5**, CD011669.

Cousins, M.J.: Acute and postoperative pain. (1989) In P.D.Wall & Melzack (Eds.), Textbook of pain (2nd ed., pp.284-305). Edinburgh: Churchill Livingstone.

Crofford, L.J. (2013) Use of NSAIDs in treating patients with arthritis. *Arthritis Res Ther*, **15 Suppl 3**, S2.

Daya, S. & Berns, K.I. (2008) Gene therapy using adeno-associated virus vectors. *Clin Microbiol Rev*, **21**, 583-593.

de Nadal, E., Ammerer, G. & Posas, F. (2011) Controlling gene expression in response to stress. *Nat Rev Genet*, **12**, 833-845.

Dominguez, G.C., Catharino, P.C.C., Casadio, C.Q.E.S., Lima, L.A.P., Tortamano, A. & Morea, C. (2012) Como preparer secções histológicas de Tecidos não descalcificados com implantes metálicos? Descrição de técnica modificada. *RPG Rev Pós Grad,* **19**, 81-7.

Eaton, M.J., Blits, B., Ruitenberg, M.J., Verhaagen, J. & Oudega, M. (2002) Amelioration of chronic neuropathic pain after partial nerve injury by adeno-associated viral (AAV) vector-mediated over-expression of BDNF in the rat spinal cord. *Gene Ther*, **9**, 1387-1395.

Fagoe, N.D., Attwell, C.L., Kouwenhoven, D., Verhaagen, J. & Mason, M.R. (2015) Overexpression of ATF3 or the combination of ATF3, c-Jun, STAT3 and Smad1 promotes regeneration of the central axon branch of sensory neurons but without synergistic effects. *Hum Mol Genet*, **24**, 6788-6800.

Fagoe, N.D., Eggers, R., Verhaagen, J. & Mason, M.R. (2014) A compact dual promoter adeno-associated viral vector for efficient delivery of two genes to dorsal root ganglion neurons. *Gene Ther*, **21**, 242-252.

Federici, T., Taub, J.S., Baum, G.R., Gray, S.J., Grieger, J.C., Matthews, K.A., Handy, C.R., Passini, M.A., Samulski, R.J. & Boulis, N.M. (2012) Robust spinal motor neuron transduction following intrathecal delivery of AAV9 in pigs. *Gene Ther*, **19**, 852-859.

Felson, D.T. (1990) The epidemiology of knee osteoarthritis: results from the Framingham Osteoarthritis Study. *Semin Arthritis Rheum*, **20**, 42-50.

Felson, D.T., Chaisson, C.E., Hill, C.L., Totterman, S.M., Gale, M.E., Skinner, K.M., Kazis, L. & Gale, D.R. (2001) The association of bone marrow lesions with pain in knee osteoarthritis. *Ann Intern Med*, **134**, 541-549.

Ferreira-Gomes, J., Adaes, S. & Castro-Lopes, J.M. (2008) Assessment of movement-evoked pain in osteoarthritis by the knee-bend and CatWalk tests: a clinically relevant study. *J Pain*, **9**, 945-954.

Ferreira-Gomes, J., Adaes, S., Mendonca, M. & Castro-Lopes, J.M. (2012a) Analgesic effects of lidocaine, morphine and diclofenac on movement-induced nociception, as assessed by the Knee-Bend and CatWalk tests in a rat model of osteoarthritis. *Pharmacol Biochem Behav*, **101**, 617-624.

Ferreira-Gomes, J., Adães, S., Sarkander, J. & Castro-Lopes, J.M. (2010) Phenotypic Alterations of neurons that innervate osteoarthritic joints in rats. *Arthritis & Rheumatism* Vol. 62, pp 3677–3685

Ferreira-Gomes, J., Adaes, S., Sousa, R.M., Mendonca, M. & Castro-Lopes, J.M. (2012b) Dose-dependent expression of neuronal injury markers during experimental osteoarthritis induced by monoiodoacetate in the rat. *Mol Pain*, **8**, 50.

Fischer, G., Kostic, S., Nakai, H., Park, F., Sapunar, D., Yu, H. & Hogan, Q. (2011) Direct injection into the dorsal root ganglion: technical, behavioral, and histological observations. *J Neurosci Methods*, **199**, 43-55.

Fishman S.M., Ballantyne J.C. & Rathmell J.P. (2010) Bonica´s management of pain. Fourth edition. Chapter 2, Pain terms and taxonomies of pain.

Forsey, R.W., Fisher, J., Thompson, J., Stone, M.H., Bell, C. & Ingham, E. (2006) The effect of hyaluronic acid and phospholipid based lubricants on friction within a human cartilage damage model. *Biomaterials*, **27**, 4581-4590.

Gibbs, S., Fijneman, R., Wiegant, J., van Kessel, A.G., van De Putte, P. & Backendorf, C. (1993) Molecular characterization and evolution of the SPRR family of keratinocyte differentiation markers encoding small proline-rich proteins. *Genomics*, **16**, 630-637.

Gibson, S.J. & Farrell, M. (2004) A review of age differences in the neurophysiology of nociception and the perceptual experience of pain. *Clin J Pain*, **20**, 227-239.

Goins, W.F., Cohen, J.B. & Glorioso, J.C. (2012) Gene therapy for the treatment of chronic peripheral nervous system pain. *Neurobiol Dis*, **48**, 255-270.

Goldberg, D.S. & McGee, S.J. (2011) Pain as a global public health priority. *BMC Public Health*, **11**, 770.

Goldring, M.B. (2000) The role of the chondrocyte in osteoarthritis. *Arthritis Rheum*, **43**, 1916-1926.

Goldring, M.B. & Otero, M. (2011) Inflammation in osteoarthritis. *Curr Opin Rheumatol*, **23**, 471-478.

Hanani, M. (2005) Satellite glial cells in sensory ganglia: from form to function. *Brain Res Brain Res Rev*, **48**, 457-476.

Handy, C.R., Krudy, C. & Boulis, N. (2011) Gene therapy: a potential approach for cancer pain. *Pain Res Treat*, **2011**, 987597.

Harel, N.Y. & Strittmatter, S.M. (2006) Can regenerating axons recapitulate developmental guidance during recovery from spinal cord injury? *Nat Rev Neurosci*, **7**, 603-616.

Havelin, J., Imbert, I., Cormier, J., Allen, J., Porreca, F. & King, T. (2016) Central Sensitization and Neuropathic Features of Ongoing Pain in a Rat Model of Advanced Osteoarthritis. *J Pain*, **17**, 374-382.

Hill, C.L., Gale, D.G., Chaisson, C.E., Skinner, K., Kazis, L., Gale, M.E. & Felson, D.T. (2001) Knee effusions, popliteal cysts, and synovial thickening: association with knee pain in osteoarthritis. *J Rheumatol*, **28**, 1330-1337.

Hill, C.L., Hunter, D.J., Niu, J., Clancy, M., Guermazi, A., Genant, H., Gale, D., Grainger, A., Conaghan, P. & Felson, D.T. (2007) Synovitis detected on magnetic resonance imaging and its relation to pain and cartilage loss in knee osteoarthritis. *Ann Rheum Dis*, **66**, 1599-1603.

Hochman, J.R., Davis, A.M., Elkayam, J., Gagliese, L. & Hawker, G.A. (2013) Neuropathic pain symptoms on the modified painDETECT correlate with signs of central sensitization in knee osteoarthritis. *Osteoarthritis Cartilage*, **21**, 1236-1242.

IASP TaxonomyWorking group: Pain terms: A current list with definitions and Notes on Usage. In Classification of chronic pain. (1994) 2nd edition.Edited by Merskey H, Bogduk N. IASP Press.

Ivanavicius, S.P., Ball, A.D., Heapy, C.G., Westwood, F.R., Murray, F. & Read, S.J. (2007) Structural pathology in a rodent model of osteoarthritis is associated with neuropathic pain: increased expression of ATF-3 and pharmacological characterisation. *Pain*, **128**, 272-282.

Jankowski, M.P., McIlwrath, S.L., Jing, X., Cornuet, P.K., Salerno, K.M., Koerber, H.R. & Albers, K.M. (2009) Sox11 transcription factor modulates peripheral nerve regeneration in adult mice. *Brain Res*, **1256**, 43-54.

Jensen, T.S., Baron, R., Haanpaa, M., Kalso, E., Loeser, J.D., Rice, A.S. & Treede, R.D. (2011) A new definition of neuropathic pain. *Pain*, **152**, 2204-2205.

Jing, X., Wang, T., Huang, S., Glorioso, J.C. & Albers, K.M. (2012) The transcription factor Sox11 promotes nerve regeneration through activation of the regeneration-associated gene Sprr1a. *Exp Neurol*, **233**, 221-232.

Julius, D. & Basbaum, A.I. (2001) Molecular mechanisms of nociception. *Nature*, **413**, 203-210.

Kartasova, T., van Muijen, G.N., van Pelt-Heerschap, H. & van de Putte, P. (1988) Novel protein in human epidermal keratinocytes: regulation of expression during differentiation. *Mol Cell Biol*, **8**, 2204-2210.

Kim, J.K., Park, S.W., Kang, J.W., Kim, Y.J., Lee, S.Y., Shin, J., Lee, S. & Lee, S.M. (2012) Effect of GCSB-5, a Herbal Formulation, on Monosodium Iodoacetate-Induced Osteoarthritis in Rats. *Evid Based Complement Alternat Med*, **2012**, 730907.

Koczot, F.J., Carter, B.J., Garon, C.F. & Rose, J.A. (1973) Self-complementarity of terminal sequences within plus or minus strands of adenovirus-associated virus DNA. *Proc Natl Acad Sci U S A*, **70**, 215-219.

Korshunova, I., Caroni, P., Kolkova, K., Berezin, V., Bock, E. & Walmod, P.S. (2008) Characterization of BASP1-mediated neurite outgrowth. *J Neurosci Res*, **86**, 2201-2213.

Lampropoulou-Adamidou, K., Lelovas, P., Karadimas, E.V., Liakou, C., Triantafillopoulos, I.K., Dontas, I. & Papaioannou, N.A. (2014) Useful animal models for the research of osteoarthritis. *Eur J Orthop Surg Traumatol*, **24**, 263-71

Lefebvre, V., Dumitriu, B., Penzo-Mendez, A., Han, Y. & Pallavi, B. (2007) Control of cell fate and differentiation by Sry-related high-mobility-group box (Sox) transcription factors. *Int J Biochem Cell Biol*, **39**, 2195-2214.

Leon, S., Yin, Y., Nguyen, J., Irwin, N. & Benowitz, L.I. (2000) Lens injury stimulates axon regeneration in the mature rat optic nerve. *J Neurosci*, **20**, 4615-4626.

Little, C.B. & Zaki, S. (2012) What constitutes an " animal model of osteoarthritis"-the need for consensus? *Osteoarthr Cart*, **20**, 216-7.

Liu, F.Y., Sun, Y.N., Wang, F.T., Li, Q., Su, L., Zhao, Z.F., Meng, X.L., Zhao, H., Wu, X., Sun, Q., Xing, G.G. & Wan, Y. (2012) Activation of satellite glial cells in lumbar dorsal root ganglia contributes to neuropathic pain after spinal nerve ligation. *Brain Res*, **1427**, 65-77.

Lohmander, S.L., Saxne, T. & Heinegard, K.D. (1994) Release of cartilage oligomeric matrix protein (COMP) into joint fluid after knee injury and in osteoarthritis. *Annls of the Rheumatic diseases*. **53**:8-13.

Lopes, C.D., Goncalves, N.P., Gomes, C.P., Saraiva, M.J. & Pego, A.P. (2017) BDNF gene delivery mediated by neuron-targeted nanoparticles is neuroprotective in peripheral nerve injury. *Biomaterials*, **121**, 83-96.

Machida, A., Kuwahara, H., Mayra, A., Kubodera, T., Hirai, T., Sunaga, F., Tajiri, M., Hirai, Y., Shimada, T., Mizusawa, H. & Yokota, T. (2013) Intraperitoneal

administration of AAV9-shRNA inhibits target gene expression in the dorsal root ganglia of neonatal mice. *Mol Pain*, **9**, 36.

Malfait, A.M. & Schnitzer, T.J. (2013) Towards a mechanism-based approach to pain management in osteoarthritis. *Nat Rev Rheumatol*, **9**, 654-664.

Martel-Pelletier, J., Barr, A.J., Cicuttini, F.M., Conaghan, P.G., Cooper, C., Goldring, M.B., Goldring, S.R., Jones, G., Teichtahl, A.J. & Pelletier, J.P. (2016) Osteoarthritis. *Nat Rev Dis Primers*, **2**, 16072.

Martel-Pelletier, J., Wildi, L.M. & Pelletier, J.P. (2012) Future therapeutics for osteoarthritis. *Bone*, **51**, 297-311.

Mason, M.R., Ehlert, E.M., Eggers, R., Pool, C.W., Hermening, S., Huseinovic, A., Timmermans, E., Blits, B. & Verhaagen, J. (2010) Comparison of AAV serotypes for gene delivery to dorsal root ganglion neurons. *Mol Ther*, **18**, 715-724.

Moran, L.B. & Graeber, M.B. (2004) The facial nerve axotomy model. *Brain Res Brain Res Rev*, **44**, 154-178.

Mow, V.C., Ratcliffe, A. & Poole, A.R. (1992) Cartilage and diarthrodial joints as paradigms for hierarchical materials and structures. *Biomaterials*, **13**, 67-97.

Nicholson, B. (2006) Differential diagnosis: nociceptive and neuropathic pain. *Am J Manag Care*, **12**, S256-262.

O'Brien, C., Woolf, C.J., Fitzgerald, M., Lindsay, R.M. & Molander, C. (1989) Differences in the chemical expression of rat primary afferent neurons which innervate skin, muscle or joint. *Neuroscience*, **32**, 493-502.

Oliveira, A.S., Felson, T.D., Reed, I.J., Cirillo, A.P. and Walker, M.A. (1995) Incidence of Symptomatic Hand, hip, and knee osteoarthritis among patients in a health maintenance organization. *Arthritis & Rheumatism*, **38**, 1134-1141.

Otis, C., Gervais, J., Guillot, M., Gervais, J.A., Gauvin, D., Pethel, C., Authier, S., Dansereau, M.A., Sarret, P., Martel-Pelletier, J., Pelletier, J.P., Beaudry, F. & Troncy, E. (2016) Concurrent validity of different functional and neuroproteomic pain assessment methods in the rat osteoarthritis monosodium iodoacetate (MIA) model. *Arthritis Res Ther*, **18**, 150.

Piel, M.J., Kroin, J.S., van Wijnen, A.J., Kc, R. & Im, H.J. (2014) Pain assessment in animal models of osteoarthritis. *Gene*, **537**, 184-188.

Polinski, N.K., Gombash, S.E., Manfredsson, F.P., Lipton, J.W., Kemp, C.J., Cole-Strauss, A., Kanaan, N.M., Steece-Collier, K., Kuhn, N.C., Wohlgenant, S.L. & Sortwell, C.E. (2015) Recombinant adenoassociated virus 2/5-mediated gene transfer is reduced in the aged rat midbrain. *Neurobiol Aging*, **36**, 1110-1120.

Pritzker, K.P., Gay, S., Jimenez, S.A., Ostergaard, K., Pelletier, J.P., Revell, P.A., Salter, D. & van den Berg, W.B. (2006) Osteoarthritis cartilage histopathology: grading and staging. *Osteoarthritis Cartilage*, **14**, 13-29.

Puljak, L., Kojundzic, S.L., Hogan, Q.H. & Sapunar, D. (2009) Lidocaine injection into the rat dorsal root ganglion causes neuroinflammation. *Anesth Analg*, **108**, 1021-1026.

Rabinowitz, J.E., Rolling, F., Li, C., Conrath, H., Xiao, W., Xiao, X. & Samulski, R.J. (2002) Cross-packaging of a single adeno-associated virus (AAV) type 2 vector genome into multiple AAV serotypes enables transduction with broad specificity. *J Virol*, **76**, 791-801.

Raivich, G. & Makwana, M. (2007) The making of successful axonal regeneration: genes, molecules and signal transduction pathways. *Brain Res Rev*, **53**, 287-311.

Rhon, D. (2008) Re: Zhang W, Moskowitz RW, Nuki G, et al. OARSI recommendations for the management of hip and knee osteoarthritis, Part II: OARSI evidence-based, expert consensus guidelines. Osteoarthritis Cartilage 2008;16:137-62. *Osteoarthritis Cartilage*, **16**, 1585; author reply 1589.

Salaffi, F., Ciapetti, A. & Carotti, M. (2014) The sources of pain in osteoarthritis: a pathophysiological review. *Reumatismo*, **66**, 57-71.

Salerno, K.M., Jing, X., Diges, C.M., Davis, B.M. & Albers, K.M. (2013) TRAF family member-associated NF-kappa B activator (TANK) expression increases in injured sensory neurons and is transcriptionally regulated by Sox11. *Neuroscience*, **231**, 28-37.

Samad, O.A., Tan, A.M., Cheng, X., Foster, E., Dib-Hajj, S.D. & Waxman, S.G. (2013) Virus-mediated shRNA knockdown of Na(v)1.3 in rat dorsal root ganglion attenuates nerve injury-induced neuropathic pain. *Mol Ther*, **21**, 49-56.

Scanzello, C.R. & Goldring, S.R. (2012) The role of synovitis in osteoarthritis pathogenesis. *Bone*, **51**, 249-257.

Scanzello, C.R., Umoh, E., Pessler, F., Diaz-Torne, C., Miles, T., Dicarlo, E., Potter, H.G., Mandl, L., Marx, R., Rodeo, S., Goldring, S.R. & Crow, M.K. (2009) Local cytokine profiles in knee osteoarthritis: elevated synovial fluid interleukin-15 differentiates early from end-stage disease. *Osteoarthritis Cartilage*, **17**, 1040-1048.

Schaible, H.G. (2012) Mechanisms of chronic pain in osteoarthritis. *Curr Rheumatol Rep*, **14**, 549-556.

Schaible, H.G. & Grubb, B.D. (1993) Afferent and spinal mechanisms of joint pain. *Pain*, **55**, 5-54.

Schaible, H.G., Richter, F., Ebersberger, A., Boettger, M.K., Vanegas, H., Natura, G., Vazquez, E. & Segond von Banchet, G. (2009) Joint pain. *Exp Brain Res*, **196**, 153-162.

Schaible H-G, Schmidt RF (1983) Responses of fine medial articular nerve afferents to passive movements of knee joint. J Neurophysiol **49** : 1118 – 1126

Schmidt, R., Schmelz, M., Forster, C., Ringkamp, M., Torebjork, E. & Handwerker, H. (1995) Novel classes of responsive and unresponsive C nociceptors in human skin. *J Neurosci*, **15**, 333-341.

Schreyer, D.J. & Skene, J.H. (1993) Injury-associated induction of GAP-43 expression displays axon branch specificity in rat dorsal root ganglion neurons. *J Neurobiol*, **24**, 959-970.

Seijffers, R., Allchorne, A.J. & Woolf, C.J. (2006) The transcription factor ATF-3 promotes neurite outgrowth. *Mol Cell Neurosci*, **32**, 143-154.

Seijffers, R., Mills, C.D. & Woolf, C.J. (2007) ATF3 increases the intrinsic growth state of DRG neurons to enhance peripheral nerve regeneration. *J Neurosci*, **27**, 7911-7920.

Sherrington, C.S. (1906) The integrative action of the nervous system. *C. Scribner and Sons*, New York.

Snider, W.D., Zhou, F.Q., Zhong, J. & Markus, A. (2002) Signaling the pathway to regeneration. *Neuron*, **35**, 13-16.

Sofat, N. & Kuttapitiya, A. (2014) Future directions for the management of pain in osteoarthritis. *Int J Clin Rheumtol*, **9**, 197-276.

Starkey, M.L., Davies, M., Yip, P.K., Carter, L.M., Wong, D.J., McMahon, S.B. & Bradbury, E.J. (2009) Expression of the regeneration-associated protein SPRR1A in primary sensory neurons and spinal cord of the adult mouse following peripheral and central injury. *J Comp Neurol*, **513**, 51-68.

Staunton, C.A., Lewis, R. & Barrett-Jolley, R. (2013) Ion channels and osteoarthritic pain: potential for novel analgesics. *Curr Pain Headache Rep*, **17**, 378.

Storek, B., Reinhardt, M., Wang, C., Janssen, W.G., Harder, N.M., Banck, M.S., Morrison, J.H. & Beutler, A.S. (2008) Sensory neuron targeting by self-complementary AAV8 via lumbar puncture for chronic pain. *Proc Natl Acad Sci U S A*, **105**, 1055-1060.

Takeda, M., Takahashi, M. & Matsumoto, S. (2009) Contribution of the activation of satellite glia in sensory ganglia to pathological pain. *Neurosci Biobehav Rev*, **33**, 784-792.

Towne, C., Pertin, M., Beggah, A.T., Aebischer, P. & Decosterd, I. (2009) Recombinant adeno-associated virus serotype 6 (rAAV2/6)-mediated gene transfer to nociceptive neurons through different routes of delivery. *Mol Pain*, **5**, 52.

Tsujino, H., Kondo, E., Fukuoka, T., Dai, Y., Tokunaga, A., Miki, K., Yonenobu, K., Ochi, T. & Noguchi, K. (2000) Activating transcription factor 3 (ATF3) induction by axotomy in sensory and motoneurons: A novel neuronal marker of nerve injury. *Mol Cell Neurosci*, **15**, 170-182.

Valdes, A.M., Suokas, A.K., Doherty, S.A., Jenkins, W. & Doherty, M. (2014) History of knee surgery is associated with higher prevalence of neuropathic pain-like symptoms in patients with severe osteoarthritis of the knee. *Semin Arthritis Rheum*, **43**, 588-592.

van der Kraan, P.M., Vitters, E.L., van de Putte, L.B. & van den Berg, W.B. (1989) Development of osteoarthritic lesions in mice by "metabolic" and "mechanical" alterations in the knee joints. *Am J Pathol*, **135**, 1001-1014.

Vicuna, L., Strochlic, D.E., Latremoliere, A., Bali, K.K., Simonetti, M., Husainie, D., Prokosch, S., Riva, P., Griffin, R.S., Njoo, C., Gehrig, S., Mall, M.A., Arnold, B., Devor, M., Woolf, C.J., Liberles, S.D., Costigan, M. & Kuner, R. (2015) The serine protease inhibitor SerpinA3N attenuates neuropathic pain by inhibiting T cell-derived leukocyte elastase. *Nat Med*, **21**, 518-523.

Vincent, T.L., Williams, R.O., Maciewicz, R., Silman, A., Garside, P. & Arthritis Research, U.K.a.m.w.g. (2012) Mapping pathogenesis of arthritis through small animal models. *Rheumatology (Oxford)*, **51**, 1931-1941.

Walk, D. & Poliak-Tunis, M. (2016) Chronic Pain Management: An Overview of Taxonomy, Conditions Commonly Encountered, and Assessment. *Med Clin North Am*, **100**, 1-16.

Watson, M.C., Brookes, S.T., Kirwan, J.R. & Faulkner, A. (2000) Non-aspirin, non-steroidal anti-inflammatory drugs for osteoarthritis of the knee. *Cochrane Database Syst Rev*, CD000142.

Weitzman, M.D. & Linden, R.M. (2011) Adeno-associated virus biology. *Methods Mol Biol*, **807**, 1-23.

Xiao, H.S., Huang, Q.H., Zhang, F.X., Bao, L., Lu, Y.J., Guo, C., Yang, L., Huang, W.J., Fu, G., Xu, S.H., Cheng, X.P., Yan, Q., Zhu, Z.D., Zhang, X., Chen, Z., Han, Z.G. & Zhang, X. (2002) Identification of gene expression profile of dorsal root ganglion in the rat peripheral axotomy model of neuropathic pain. *Proc Natl Acad Sci U S A*, **99**, 8360-8365.

Yoshida, A., Morihara, T., Matsuda, K., Sakamoto, H., Arai, Y., Kida, Y., Kawata, M. & Kubo, T. (2012) Immunohistochemical analysis of the effects of estrogen on intraarticular neurogenic inflammation in a rat anterior cruciate ligament transection model of osteoarthritis. *Connect Tissue Res*, **53**, 197-206.

Yu, H., Fischer, G., Ferhatovic, L., Fan, F., Light, A.R., Weihrauch, D., Sapunar, D., Nakai, H., Park, F. & Hogan, Q.H. (2013) Intraganglionic AAV6 results in efficient and long-term gene transfer to peripheral sensory nervous system in adult rats. *PLoS One*, **8**, e61266.

Yu, H., Fischer, G. & Hogan, Q.H. (2016) AAV-Mediated Gene Transfer to Dorsal Root Ganglion. *Methods Mol Biol*, **1382**, 251-261.

Zimmermann, M. (1983) Ethical guidelines for investigations of experimental pain in conscious animals. *Pain*, **16**, 109-110.

Appendix

Solutions preparation-general reagents

- **Collagenase** – 2,5mg of Type II collagenase from Clostridium histolyticum (Sigma-Aldrich ®) diluted in 100 μl of 0,9% saline.
- **Tyrode´s solution-** 6,8g of sodium chloride (N_aCl), 0,40g of potassium chloride (KCL), 0,32g of hydrated magnesium chloride ($MgCl_2.6H_2O$), 0,1g of hydrated magnesium sulphate ($MgSO_4.7H_2O$), 0,17g of hydrated sodium dihydrogenophosphate ($NaH_2PO_4.H_2O$), 1,0g of glucose and 2,2g of sodium hydrogenocarbonate ($NaHCO_3$); add distilled water up to the final volume of 1000 ml.
- **Sucrose solution 30% in Phosphate buffer 0,1M-** 30g of sucrose diluted in phosphate buffer 0,1M to final volume of 1000 ml.
- **Phosphate buffer 0,4M (stock solution)-** 26,2g of hydrated sodium dihydrogenophosphate ($NaH_2PO_4.H_2O$), 140g of potassium hydrogenophosphate (K_2HPO_4) diluted in distilled water up to the final volume of 2500 ml. (pH between 7,2 and 7,4).
- **Phosphate buffer saline 0,1M (PBS)-** 250 ml of phosphate buffer 0,4M and 9g of sodium chloride (N_aCl) diluted in distilled water up to 1L.
- **Phosphate buffer saline 0,1M with Triton X-100 (PBST)-** 250 ml of phosphate buffer 0,4M and 9g of sodium chloride (N_aCl) diluted in distilled water up to 1L. Add 12 ml of Triton-X-100 at 25%.
- **Solution A of Methylmethacrylate** – 75 ml of Methylmethacrylate and 25 ml of Dibutyl phthalate to a final volume of 100 ml.
- **Solution B or 1% solution of Methylmethacrylate -** 75 ml of Methylmethacrylate and 25 ml of Dibutyl phthalate and 1g of Benzoyl peroxide to a final volume of 100 ml.
- **Solution C or 2,5% solution of Methylmethacrylate -** 75 ml of Methylmethacrylate and 25 ml of Dibutyl phthalate and 2,5g of Benzoyl peroxide to a final volume of 100 ml.
- **0,02% Fast Green-** 0,02g of Fast green diluted in distilled water up to 100 ml.

- **0,5% Safranin-** 0,5g of Safranin diluted in distilled water up to 100 ml.